A New Model for the Living Cell: A Summary of the Theory and Recent Experimental Evidence in Its Support

GILBERT N. LING

Department of Molecular Biology, Division of Neurology, Pennsylvania Hospital, Philadelphia, Pennsylvania

Introduction

It is generally acknowledged that living organisms, although vastly complex, can eventually be understood in terms of basic principles derived from studies of the simple inanimate world. The primary function of a biologist is thus not so much to deduce basic principles—that belongs to physics—but to understand how these principles apply in a unique complex system. The most logical time to begin fundamental biological research, therefore, would be when men have achieved complete understanding of the physical world. Then one could be certain that the foundations of his reasoning would be sound. Since this has not been the case—investigations of living matter are as old as the study of the inanimate world—the student of biology must be doubly cautious in accepting assumptions presented as facts. Thus, for example, in the writing of textbooks, what *could be* is often transformed into what *is*. For this reason the student must constantly reexamine the major premises no matter how popular or venerable, using both up-to-date knowledge of the physical sciences and advanced tech-

nology that was not available to investigators of previous days. The present review begins with such a reevaluation of the basic assumptions of an old and venerable concept, the membrane theory. After discussing some of the difficulties in this concept, it goes on to summarize both theoretical aspects of and experimental evidence for an alternative model of the living cell.

I. The Membrane Theory

A. History

About 90 years ago, H. Pfeffer, struck by the similarity between the osmotic behavior of living cells and that of an aqueous solution enclosed in a semipermeable membrane, propounded the membrane theory (Pfeffer, 1921). According to this view, the outermost layer of any living cell consists of a membrane which is a universal rate-limiting barrier to the traffic of water and all solutes between the cell interior and the external environment. A second implicit assumption was that there is no significant interaction between the cell proteins which constitute 15–25% of the cell weight and the cell water which makes up almost all the rest (75–85%) (Ling, 1962). Thus the water in the cell was postulated to be essentially the same as in any dilute salt solution. On the basis of these assumptions, the problems of water and solute distribution as well as the maintenance of cell volume can be expressed in terms of one all-encompassing parameter, the *membrane permeability*. Thus the degree of cell swelling in a medium containing a particular solute reflects the permeability or impermeability of the cell membrane to this solute (De Vries, 1885; Hamburger, 1889).

In the following six decades much effort was devoted to discovering the properties of this cell membrane that allowed it to determine not only the rates of entry and exit of water and solutes into and out of the cell but also their steady levels within the cell. At the turn of the century, Overton, using osmotic methods such as cell swelling, studied the relative permeability of many solutes (Overton, 1899, 1907). A parallel between the permeability of many nonelectrolytes and their oil/water distribution coefficients led him to suggest that the cell membrane consists of a continuous lipid layer. He further suggested that the transport of nonlipid-soluble solutes such as sugars, amino acids, and ions was promoted by "adenoid" or secretory activity. In 1933, Collander and Bärlund confirmed Overton's findings by measuring solute permeation into plant cell sap. They found, however, that the high permeability of water was not compatible with its low oil/water distribution coefficient, leading them to postulate the existence of small aqueous channels in the lipid membrane that permit water (and other small molecules) to pass through (mosaic membrane theory) (Collander and Bärlund, 1933). The discovery, also in the 1930's, that the surface tension of cells is far less than that at an oil/water interface led to the suggestion of a

protein covering for the lipid layer (Cole, 1932; Davson and Danielli, 1952). Ruhland and Hoffman (1925) first suggested that the cell membrane may be sievelike, selectively admitting some ions but not others (Ruhland and Hoffman, 1925; see also Mond and Netter, 1930). The sieve theory reached the height of its development in the version presented in 1941 (Boyle and Conway, 1941): The critical pore size was postulated to be such that the permeabilities of both cations and anions could be explained. Small cations like K^+ ion and H^+ ion were considered permeable, while the large cations, Na^+, Ca^{++}, and Mg^{++} were not. Small anions like Cl^- and OH^- were permeable but not larger anions like ATP, CrP, and hexose phosphates. Not only did this theory present a unified interpretation for the distribution of all types of ions, it also provided the molecular basis essential to Bernstein's membrane theory of cellular electric potential. If one considered the small pores of Boyle and Conway the same as those postulated by Collander and Bärlund one could envisage an internally consistent interpretation for the permeability of nearly all solutes and water.

This state of apparent harmony between the membrane theory and the experimental facts, however, did not long survive the publication of Boyle and Conway's theory (1941).

About the same time Heppel (1940) and Steinbach (1940) demonstrated that muscle cells are in fact permeable to Na^+ ion. This was construed by most as a refutation of Boyle and Conway's specific theory. In order to account for the low steady level of Na^+ ion in the cell in spite of its constant inward diffusion, the remedial Na^+-ion pump hypothesis was advanced (Dean, 1941; Krogh, 1946; Hodgkin, 1951). The reviewer feels, however, that the findings of Heppel and of Steinbach have greater significance than is usually recognized: (1) Thus, increasing the Na^+-ion concentration of the external medium leads to cell shrinkage; therefore, this ion satisfies the criterion on the basis of the membrane theory, of an impermeant solute. The demonstration that it is permeable shows such swelling and shrinking effects cannot be used as a gauge of permeability. This invalidates the basic assumption involved in the widespread use of osmotic behavior as a measure of membrane permeability. (2) If the Na^+ ion enters the cell via the aqueous channels (that the bulk of Na^+ ion entering muscle cells does not show competition supports this; see Fig. 21; Ling and Ochsenfeld, 1965), these channels must also be wide enough to permit the passage of nonelectrolytes like glycerol, erythritol, and so forth. Such compounds are far less soluble in lipids than in water. Thus they cannot be assumed to enter the cell via the lipid layer rather than the aqueous channels. If they do enter via the aqueous channels, the observed linear correlation between the oil/water distribution coefficient and the permeability of nonelectrolytes (Overton, 1907; Collander, 1949) cannot be based on permeation through a lipid membrane. (3) According to the theory of Boyle and Conway, hydrated Na^+, Ca^{++}, Mg^{++} ions, as well

as ATP, CrP, and hexose phosphates are all impermeable because they are larger than the pores. However, Na^+, Ca^{++}, and Mg^{++} ions have all been shown to be permeable (Ling, 1962). What then prevents ATP, CrP, and hexose phosphates from diffusing out? Since according to the membrane theory these are the impermeant anions in a Donnan equilibrium, their outward diffusion also leads to a collapse of the resting potential (Boyle and Conway, 1941).

These are some of the problems raised by the demonstration of Na^+-ion permeability; they cannot be remedied merely by the postulation of a Na^+ pump. Even more difficulty is raised by the demonstration that cells are permeable to much larger molecules than Na^+ ions: There is increasing evidence that both proteins and other macromolecules can enter and exit from cells (Avery *et al.,* 1944; Dawson, 1966; McLaren *et al.,* 1960; Zierler, 1958; Ryser, 1968). Thus, Dawson (1966) has shown that enzymes diffuse from isolated intact chicken muscles. Ryser studied the entry of I^{131}-labeled serum albumin and many other proteins including poly-L-lysine and poly-D-lysine showing that all these molecules enter cells with rates generally proportional to their molecular weights.[1]

Thus the membrane theory, in its present state, is beset with internal inconsistencies. There are, however, more fundamental questions that must be raised concerning the general validity of the membrane theory: (1) Does the resting cell produce energy at a rate sufficient to provide for all the necessary "pumps"? (2) Is there truly no significant interaction between cell proteins and cell water? (3) Is the cell membrane a universal rate-limiting barrier to the traffic of water and other solutes between the cell interior and its external medium?

By making use of technology not available until very recently, critical experi-

[1] One mechanism offered for the entry of proteins into cells is based on the concept of pinocytosis; i.e., the cell actually phagocytizes droplets of its external medium containing macromolecules (Bennett, 1956; Holter and Holtzer, 1959). There are a number of difficulties associated with this concept: (1) According to current concepts of pinocytosis, the macromolecules phagocytized, although within the cells, are actually outside of the cytoplasm because there is a continuous plasma membrane surrounding the vesicle. Unless there is entry of the substance into the cell from this vesicle, however, it is difficult to understand how macromolecules can have any physiological action on the cell, such as, for example, the effect of DNA on capsule formation in *Pneumococcus* (Avery *et al.,* 1944). If the substances enter the cells by a "melting away" of the plasma membrane, the consequence of pinocytosis would be the creation of a nondiscriminatory route for the entry of all solutes into the cell. If this is the case, it is difficult to explain why poly-D-lysine enters more rapidly than poly-L-lysine (Ryser, 1968) into living cells, as well as the correlation between the rate of entry of nonelectrolytes and their oil–water partition coefficients. (3) Metabolic poisons such as iodoacetate, NaF, 2,4-dinitrophenol, and cyanide, which inhibit phagocytosis, do not inhibit the entry of I^{131}-labeled serum albumin into living cells (Ryser, 1968). (5) Last, in what way can the cell prevent continued pinocytosis from ingesting and depositing an ever-increasing amount of external proteins in the cell? Must we postulate protein pumps?

ments have been carried out that have provided answers to these questions. One may add that, had it been technically feasible, some of these experiments should have been carried out shortly after Pfeffer presented the membrane theory some 90 years ago.

B. The Energy Requirement of the Necessary Pumps

Shortly after the Na^+ pump was postulated, no less than four sets of experiments (excluding the reviewer's) were published, all comparing the minimum energy need of the Na^+ pump in frog sartorius muscles with the maximum energy available (Conway, 1946; Levi and Ussing, 1948; Harris and Burn, 1949; Keynes and Maisel, 1945). Conway (1946), as well as Levi and Ussing, regarded the energy consumption as being too high for the cell to cope with. However, Conway's Na^+-ion efflux data were indirectly deduced and might thus be subject to question. The data of Levi and Ussing (1948), Harris and Burn (1949), and Keynes and Maisel (1945) are more or less consistent with one another and show a minimum requirement of about 20% of the total energy output. These figures were derived on the assumption that all the energy from glucose oxidation is converted to a form suitable for consumption by the pump at 100% efficiency and that the pump itself is also 100% efficient. Since neither assumption is likely to be true, these figures themselves indicate a failing in the pump concept (Ling, 1955).

Because of the crucial importance of the issue, I reexamined the energy problem in two ways:

(1) *The energy requirement of the Na^+ pump at 0°C. in muscles poisoned with iodoacetate and pure nitrogen.* Arrest of oxidation and glycolysis does not significantly alter the steady level of Na^+ and K^+ ion in frog muscle cells (0°C.) for as long as 7 hours (Ling, 1962, p. 200). During this time the efflux of Na^+ ion continues at a rate not slower than that of the unpoisoned control muscle (Ling, 1962, p. 198). Without oxidation and glycolysis the energy sources of the muscle cells are limited to its store of ATP and creatine phosphate. Comparing the maximum energy available from the hydrolysis of these compounds with the minimum energy need calculated for pumping on the basis of the measured resting potential, the intracellular Na^+-ion concentration, and the Na^+-ion efflux rate,[2] I reached the conclusion that the minimum energy need is

[2] I have been asked a number of times whether the Na^+-ion efflux value used in the computation might be an overestimation. Thus for normal muscles at 0°C, I gave an efflux rate of 1.76×10^{-11} mole/cm.^{2}/sec. (in contrast to the value of Harris of 4.7×10^{-12} mole/cm.^{2}/sec., 123). The rate of efflux from poisoned muscle was higher ($3.9–8.73 \times 10^{-11}$ mole/cm.^{2}/sec.).

Harris' value was based on an efflux curve not significantly different from mine (compare Harris, 1950, Fig. 2 with Fig. 11.29 in reference Ling, 1962). However, he discounted

1500–3500% of the maximum available energy, again assuming 100% efficiency (Ling, 1962, p. 211).

(2) *The energy requirement of the Na,+, Ca++, and Mg++ pumps in resting frog muscle cells.* At the time Na^+ ion was demonstrated to be permeable, it was considered an exception and the Na^+ pump was postulated. However, it was not long before it was discovered that no two ions distribute themselves between the inside and the outside of the cell with the same Donnan ratio, and all are permeable (Ling, 1955).

To explain this phenomenon on the basis of the membrane theory, more pumps must be postulated with, however, the same maximum energy source (already overstretched for the Na^+ pump alone). Using the data available in the literature I calculated that the Na^+, Ca^{++}, and Mg^{++} pumps alone would consume no less than 350% of the total maximum available energy of a resting frog muscle (Ling, 1965b). To this must be added pumps to maintain the levels of all the other solutes (HCO_3^-, Cl^-, amino acids, and so forth) which are not distributed between the cell and its surrounding medium according to thermodynamic equilibrium.

---

the early fast fraction (15–20 minutes) as being attributable to efflux from the extracellular space. Our subsequent study of Na^+-ion efflux from isolated single muscle fibers, however, shows that this fraction cannot be in the extracellular space. Thus it takes less than 1 second to wash away the adhering solution in this preparation—but these fibers still possess a similar fast fraction (see Fig. 11.4, Ling, 1962) (Curves obtained by Horowicz and Hodgkin (Horowicz and Hodgkin, 1957) from single muscle fibers were apparently exponential; however, the setup used by these authors did not allow points before the first 10 minutes of washing; after that they could obtain readings at only about 10-minute intervals. Under such conditions the curvature is lost).

In all the estimations of energy balance quoted above, it had been taken for granted that the slow flat portion of the efflux curve represents the Na^+ ion pump. However, the evidence quoted in Section III, B,4 gives us considerable reason to equate the slow fraction in the Na^+-ion efflux with exchange of the adsorbed fraction. If this is the case (for additional evidence, see Ling, 1962), the fast fraction actually represents the rate of efflux of the free Na^+ ion into the environment and should be used for the rate of pumping (Ling, 1962, Chapt. 11; Ling, 1966a).

In conclusion, I might point out that the method I used to derive the rate of efflux was chosen to give a conservative estimate. A small bundle of muscle fibers was dipped for a time interval (about 3 minutes) in an isotope-labeled solution. The tissue was then quickly mounted on the washout apparatus and an efflux curve obtained for the succeeding 100–200 minutes by which time the curve had become exponential. This exponential part of the curve was then extrapolated to the ordinate to give an estimate (in actuality too small) of the amount of Na^+ ion that entered the cell during the 3-minute incubation. Since there was no change in the total Na^+-ion concentration during this time, the influx rate and efflux rate must have been equal. The rate of pumping was then derived from this figure.

C. The Physical State of Water in the Living Cell

Evidence has been gathering at a rapid rate which shows that the cell water is in a different state than the water in a dilute salt solution. Since this subject will be discussed at length in a following section, we shall only point out here that there are two lines of evidence pointing to the above conclusion: (1) the abnormal freezing pattern of water in the living cell (Chambers and Hale, 1932; Rapatz and Luyet, 1958; Ling, 1967c) when compared to that of normal water or the water in a dilute salt solution (Ling, 1966b); and (2) The abnormal nuclear magnetic resonance (NMR) spectra (Chapman and McLaughlan, 1967; Fritz and Swift, 1967) obtained from the water in living cells.

D. Is the Cell Membrane a Universal Rate-Limiting Barrier to the Intracellular-Extracellular Traffic of Water and All Solutes?

Recently the reviewer has presented a technique, influx profile analysis, that provides a means of determining the rate-limiting step in the traffic of water or solutes between the cell and its environment (Ling, 1966a; see Fig. 1). In brief, the fractional uptake of a labeled material t seconds after the introduction of a cell into a solution containing the isotope is plotted against the square root of t. The profile has specific features depending on the rate-limiting step. Thus, if the rate-limiting step is in the cell membrane, the curve is sigmoid in shape (Fig. 1A). On the other hand, if the solute diffuses with a more-or-less uniform rate throughout the entire cell including the cell membrane (bulk-phase-limited diffusion), the initial part of the curve is essentially a straight line (Fig. 1B). This technique can be most usefully applied to single cells. Figure 2 shows the influx profile for the entry of tritium hydroxide–labeled water into a single frog ovarian egg (Ling *et al.*, 1967). The solid line, passing through the points has been theoretically calculated to represent bulk-phase-limited diffusion. This shows that the cell membrane is no more resistant to water movement than the cytoplasm. The overall diffusion coefficient ranges from one-half to one-third of the diffusion coefficient of tritium hydroxide in a 0.1 N salt solution.

This set of experiments disproves one of the basic tenets of the membrane theory with respect to water. However, water is by no means the only substance whose movement is not limited by the membrane. Fenichel and Horowitz have demonstrated that the efflux of many nonelectrolytes from frog muscles is also bulk-phase limited (Fig. 3; Fenichel and Horowitz, 1963). This study included many of the same nonelectrolytes investigated by Overton and by Collander. Thus, it appears that the "membrane" permeability investigated by these authors was, in some cases at least, the permeability of the bulk of the protoplasm.

Summarizing, we can now state that (1) the resting cell does not command enough energy to operate all the pumps necessary in terms of the membrane

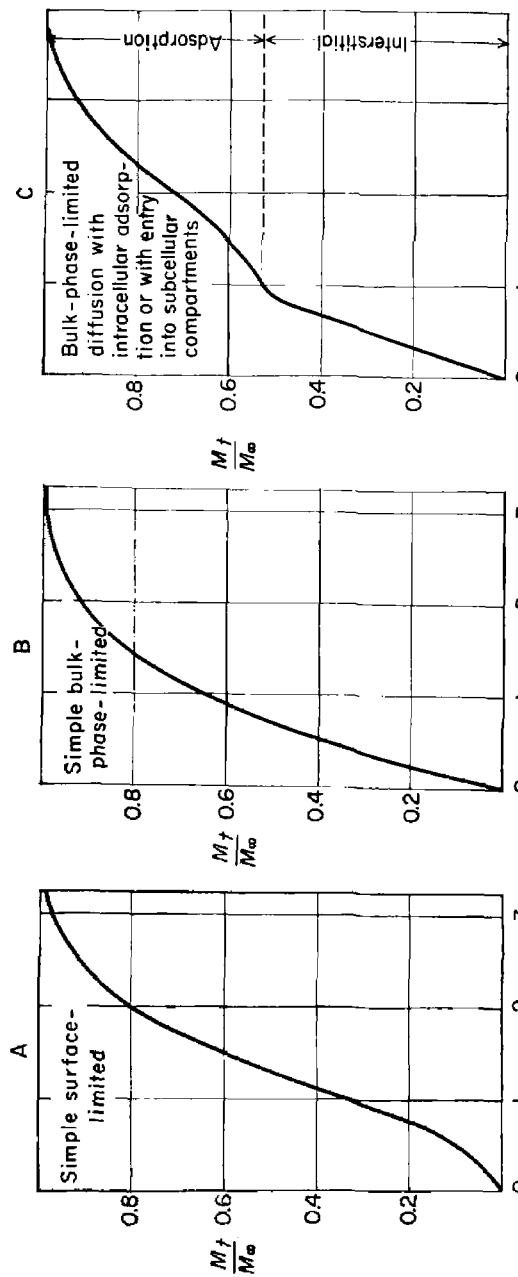

FIG. 1. The time course of influx of a labeled substance into model systems with rate-limiting steps as indicated on each chart. The "influx profiles" are theoretically calculated. The ordinate represents the uptake, M_t, of the labeled material at time t as a fraction of the final amount of the material in the system ($M\infty$). The abscissa represents the square root of t (Ling, 1966a, by permission of *Annals of the New York Academy of Sciences*).

theory to maintain the observed assymetrical solute distribution; (2) the cell water is not normal as postulated by the membrane theory, and (3) the cell membrane is not a universal rate-limiting barrier to the traffic of water and solutes between the cell and its environment.

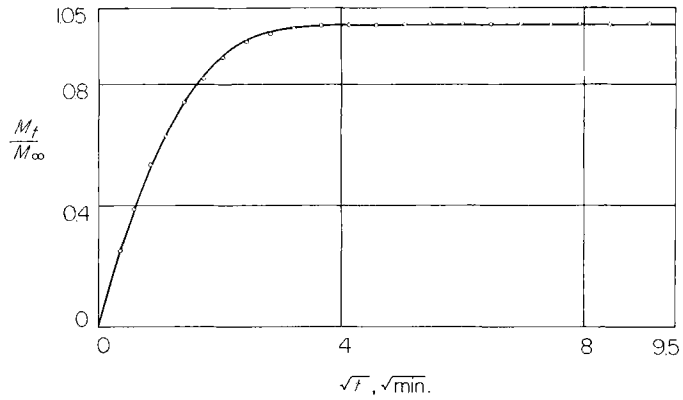

FIG. 2. Influx profile of THO-labeled water into egg clusters. Data from efflux study converted into an influx time course using the "inversion method." The curve passing through the points is theoretically computed on the basis of simple bulk-phase-limited diffusion (Ling *et al.*, 1967, by permission of *The Journal of General Physicology.*)

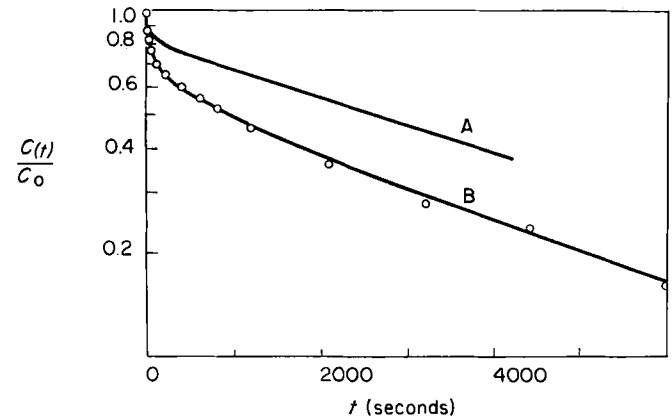

FIG. 3. The time course of labeled thiourea efflux from a frog sartorius muscle. Efflux of C^{14}-labeled thiourea was assayed by agitating muscles previously equilibrated with thiourea, in different portions of nonlabeled Ringer solution, the activity of which was then assayed. Curve A is theoretically calculated for membrane-limited diffusion and does not fit the data. Curve B, which fits the data nearly perfectly, was calculated theoretically on the basis of bulk-phase-limited diffusion. C_t is the concentration of labeled thiourea at time t in cells; C_0 is that at t equals 0 (Fenichel and Horowitz, 1963, by permission of *Acta Physiologica Scandinavica*).

Taken together, this evidence is very strongly against the membrane pump theory. Therefore, we have little choice other than to seek a new model of the living cell both to interpret the vast amount of data already accumulated and to guide future research.

II. An Interesting Clue in the Search for a Better Model of the Living Cell

Figure 4 shows an electron micrograph by Starr and Williams of a flagellum from the Congo diphtheroid bacillus (Starr and Williams, 1952). The dry matter of such flagella is virtually pure protein (Weibull, 1960). Isolated flagella

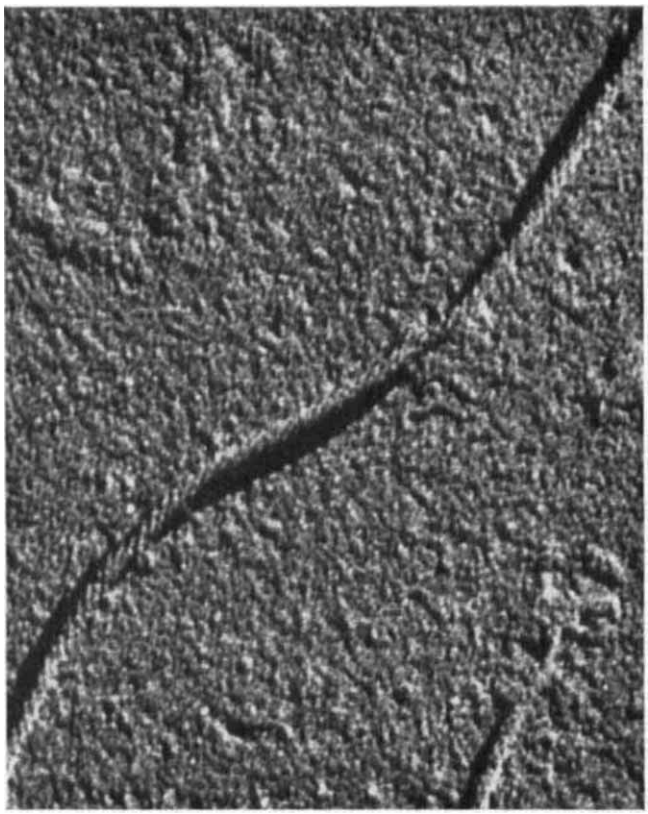

FIG. 4. Electron micrographs exhibiting the helical fine structure of flagellar material from the Congo diphtheroid bacterium. The structure is that of a left-handed, triple-stranded helix with a diameter of 19 mμ and an axial periodicity of 50 mμ 100,000 × (Starr and Williams, 1952, by permission of *Journal of Bacteriology*).

can be reversibly precipitated by ammonium sulfate and behave in many ways like homogeneous protein molecules. There is no membrane cover. The isolated flagellum apparently possesses neither ATPase nor any other enzyme. It is directly connected to the protoplasm at a subcellular structure called the basement granule (Weibull, 1960). In spite of its structural simplicity, this protein–water system is capable of undergoing spiraling movement, thus providing the driving force for the mobility of the bacterium (Holwill and Burge, 1963).

The bacterial flagellum is an illuminating example of the fundamental capabilities of protoplasm, with control and energization occurring at the basement granule away from the body of flagellum itself (Astbury, 1951). Thus, this system illustrates the transmission of information and energy for long distances along a protein–water system.

It is, according to the association–induction hypothesis, this fundamental ability of organized protein–water–ion systems to undergo reversible changes between metastable equilibrium states that distinguishes this and many other types of protoplasm from the inanimate world. The cell owes both its functional coherence and its discontinuity from the external environment not to a lipid membrane but to the unique properties of the protein–water system, just as the naked flagellum, a permanent organelle in an aqueous environment, is functionally coherent and discontinuous with its environment.

III. The Association–Induction Hypothesis

The association-induction hypothesis considers the maintenance of the pattern of solute distribution to reflect the properties of the entire protoplasm (Ling, 1962, 1964b, 1965a,b, see also Bütschli, 1894).

It is well known that the water content of a living cell is more or less constant. It is also generally accepted that water distribution represents an equilibrium state, which means that the free energy of water within the cell is equal to the free energy of water outside the cell. Therefore, within a unit time interval, the number of water molecules entering the cells exactly equals the number of water molecules leaving the cell. To maintain this steady level of water, the cell does not expend energy.

The association–induction hypothesis maintains that the steady levels of *all* the solutes in the living cell also represent equilibrium states, or rather metastable equilibrium states. A metastable equilibrium state is a true equilibrium state, only its maintenance is somewhat precarious much like the case of a narrow block of wood standing on its edge.

In the following review, I shall deal specifically with K^+ and Na^+ ion, with

the understanding that the mechanisms involved in their distribution and control are basically all similar for other solutes.

A. The Molecular Mechanism for Solute Distribution in Living Cells: Theoretical Aspects

According to the association–induction hypothesis (see also Fischer and Moore, 1908; Troschin, 1958), intracellular solutes exist in two states: (1) solution in the cell water and (2) adsorption onto cell proteins. Since the amount of solute in the first state depends on the state of the water in the cell, an important part of our discussion of solute distribution will be a consideration of the state of water in the living cell. Following this we will go on to consider the effect of the state of water on the distribution of solutes, and finally we will deal with the specific adsorption sites for the solute. We will first consider the theoretical aspects of these problems followed by a discussion of the experimental evidence in support of the model.

1. The Effect of the Protein on the State of Water in Living Cells

Water molecules possess a strong permanent dipole moment (1.83×10^{-18} e.s.u.) as well as a high polarizability (1.44×10^{-24} cm.), hence a great propensity to form strong induced dipoles (Ling, 1962, p. 65). A simple calculation shows that the electrostatic interaction of water molecules with an electrical charge carried, for example, by an ion extends beyond the first layer of water molecules surrounding the ion to a number of additional layers. Polar compounds like titanium dioxide also interact with water. Experimentally, Harkins has shown that the heat of desorption of the first layer of water molecules from the surface of titanium dioxide is 6550 cal./mole higher than from quartz. For the second layer, it is 1380 cal./mole higher; for the third layer, 220 cal./mole higher; and for the fourth layer, 71 cal./mole higher (Harkins, 1945). Protein, similar to titanium dioxide, bears an abundance of polar groups. In muscle cells the average chain-to-chain distance between protein molecules is only 16.9 A., less than the thickness of seven layers of water molecules. All or nearly all of the water in a typical resting cell may thus be under the polarizing influence of the ionic and hydrogen-bonding groups of the proteins and exist as polarized multilayers (Ling, 1962, Chapt. 2, 1965a; 1966b; 1967c). Further, this polarization must orient the water molecules in directions that are determined by the structure and orientation of the proteins.

In such a system, the freedom of motion of the individual water molecules is more constrained than in normal water, this restriction being most prominent in rotational motion. The degree of restriction falls off gradually with the distance from the protein surfaces as illustrated in the diagram shown in Fig. 5, in which the length of the curved arrows indicates the degree of rotational freedom.

2. *The Entropic Exclusion of Multiatomic or de Facto Multiatomic Solutes from Polarized Water*

In an aqueous medium, Na^+ ion acquires at least one layer of water of hydration; i.e., water molecules that are strongly polarized under the influence of the electric charge of the ion. This hydrated ion behaves as a single unit, hence it is *de facto* multiatomic. Such a molecule possesses many modes of rotational mo-

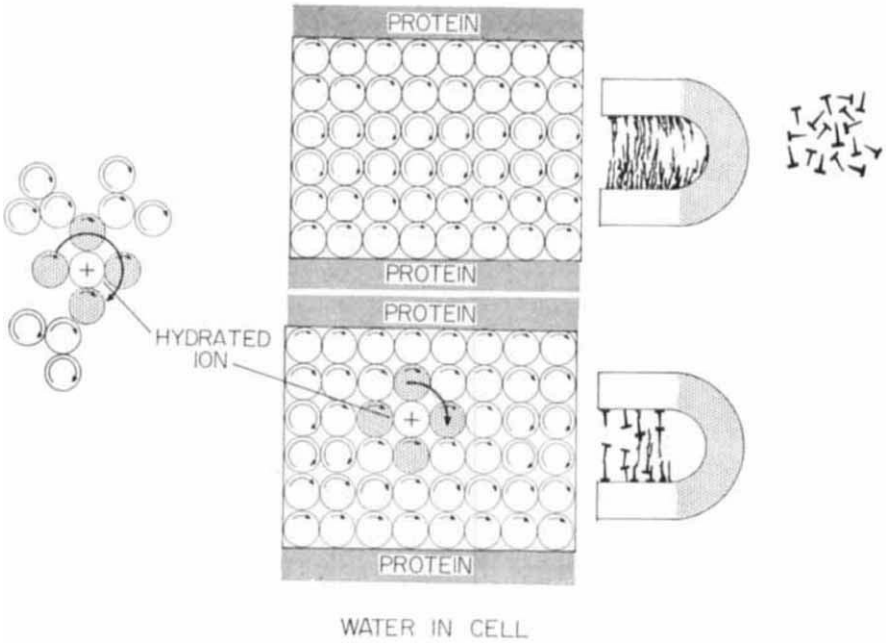

FIG. 5. Diagrammatic representation of the adsorption of water molecules as polarized multilayers on proteins. On entering such a system, the hydrated ion shown to the left suffers severe rotational restriction. A simple model of this effect is shown on the right where the restricted orientation of small nails in the field of horseshoe magnet filled with iron filings is shown.

tion. In fact, rotational entropy, which is a measure of the rotational freedom of the molecule, constitutes the major part of the entropy of such an ion in an aqueous medium.

When a hydrated ion, such as Na^+ ion, is introduced into the cell where the bulk of the water is polarized into multilayers, it suffers a restriction of its rotational movement in a manner analogous to the loss of freedom in the orientation of small nails (Fig. 5) introduced into the iron filing–filled space of a horseshoe magnet. The result of this rotational restriction is a lowered entropy. At equilibrium the distribution of a solute between a system containing oriented

water and a normal aqueous medium is determined by the difference in the standard free energy, of the solute in the two media. The $\triangle F^\circ$, in turn, is the sum of an energy term[3] and an entropy term. The energy does not differ very much between the two systems. A lowered entropy of the Na^+ ion in the cell water means a lowered $\triangle F^\circ$ and thus a lower equilibrium concentration of Na^+ ion in the polarized water.

3. *The Molecular Mechanism of Ionic Adsorption*

As far back as 1908, Fischer and Moore suggested that selective K^+-ion accumulation might result from adsorption on cell colloids (Fischer and Moore, 1908). In 1951 and 1952, the reviewer suggested that the β- and γ-carboxyl groups carried by the aspartic and glutamic acid side chains could offer anionic sites for the adsorption of K^+ as well as Na^+ ion (Ling, 1951, 1952). The hydrated diameter of the K^+ ion is considerably smaller than that of the hydrated Na^+ ion. Following Coulomb's law, the electrostatic interaction of K^+ ion with the negatively charged carboxyl groups would be greater than that of larger hydrated Na^+ ion. By taking into account the profound reduction of dielectric constant in the immediate neighborhood of an ion (the dielectric saturation phenomenon), a selectivity of K^+ ion over Na^+ ion of the order of 10 to 1 can be theoretically calculated. In support of this hypothesis, the reviewer drew an analogy between the newly developed ion exchange resins and the living cell. By introducing anionic groups and fixing them on a three-dimensional network, selective accumulation of K^+ over Na^+ ion was achieved in the resin.

In the years following, additional knowledge was gained in the field of ion-exchange resin technology. It was demonstrated that such resins do not always selectively accumulate K^+ ion over Na^+ ion. Thus, resins bearing strongly acidic groups (low pK) prefer K^+ ion over Na^+ ion. However, for resins bearing weakly acidic groups (high pK), the reverse is the case (Bregman, 1953). This fact and the theoretical and experimental work of Eisenman, Rudin, and Casby on glass electrodes (Eisenman *et al.*, 1957) led to a complete revision of the earlier model (Ling, 1960). It became apparent that the pK value primarily reflects the electron density of the acidic group. To put this concept in manipulatable form, the *c*-value was introduced. This parameter is rigorously defined elsewhere (Ling, 1962, p. 57). For simplicity, it may be mentioned that a high *c*-value (i.e., approximately -1 A.) corresponds to a high pK value (e.g., acetic acid, $pK = 4.75$). A low *c*-value (i.e., -5 A.) on the other hand, corresponds to a low pK value (e.g., trichloroacetic acid, $pK < 1.0$).

[3] More correctly this term should refer to enthalpy or heat content H which is related to the energy U by the relation: $H = U + PV$, where P is the pressure and V is the volume of the system. Since in a liquid system, volume changes are small and only changes of H and U are significant in our discussion, the more familiar *energy* is used here.

With the c-value defined, it becomes possible to calculate the total interaction energy between a specific cation (e.g., K^+ or Na^+ ion) and an oxyacid group (such as a carboxyl group) of a certain c-value, when the cation is separated from the oxyacid group by zero, one, two, or three water molecules (see Fig. 6).

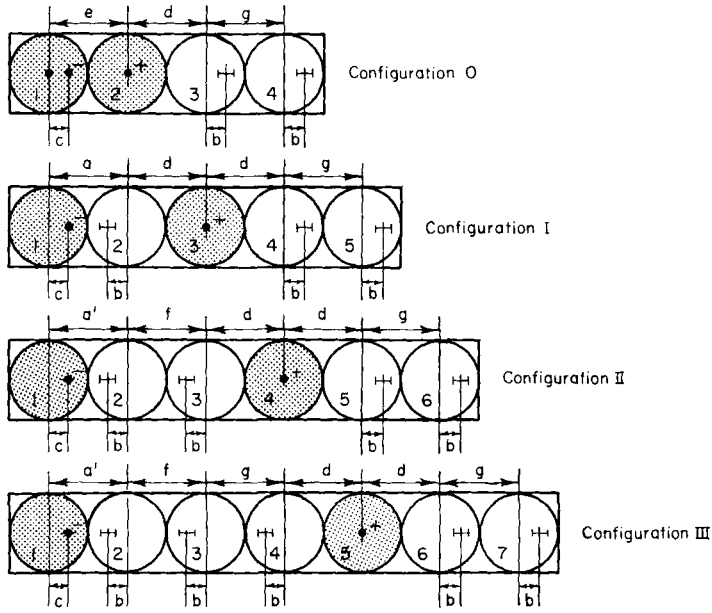

FIG. 6. The linear model. The shaded circle on the left in each configuration represents the negatively charged oxygen atom of an oxyacid (e.g., carboxyl) and the shaded circle on the right represents its counter-action. Open circles represent water and the various letters denote distances used in the computations. Reprinted by permission of the publisher from: Gilbert N. Ling, "A Physical Theory of the Living State" (Waltham, Massachusetts: Blaisdell Publishing Company, a Division of Ginn and Company, 1962) p. 61.

From these results, the dissociation energy of different alkali-metal ions can be determined as a function of the c-value (as well as the polarizability) of the anionic group. Figure 7 shows the results of such a calculation. As the c-value increases, the order of preference of the anionic group for the five alkali-metal cations goes through 11 permutations. At the lowest c-value the sequential order is $Cs > Rb > K > Na > Li$ while at the highest c-value the order is completely reversed. These theoretically calculated sequential order changes are similar to sequential order changes observed experimentally by Eisenman (Eisenman, 1961; Fig. 8) in the relative preference of glass electrodes of varying composition for the alkali-metal ions.

One significant conclusion to be drawn from the results of these calculations

is that a small change of the c-value can significantly alter the relative preference of an acidic group for K^+ over Na^+ ion. When the c-value change is large enough, the order of preference can actually be reversed. This point will be discussed again in Section III, D,7.

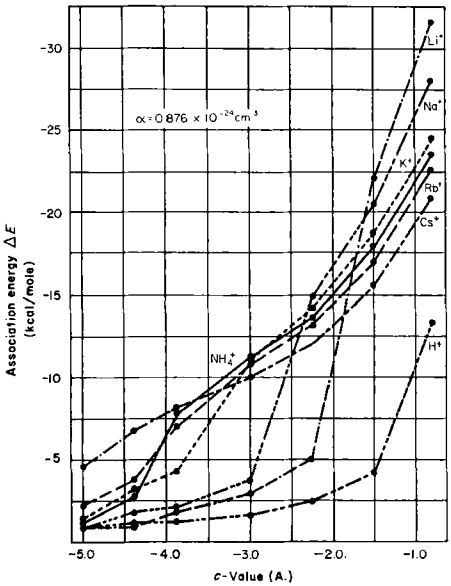

FIG. 7. The computed dissociation energy of various cations as a function of the c-value. A polarizability of 0.87×10^{-24} cm.^{3} has been assumed for the fixed anionic group. Reprinted by permission of the publisher, from Gilbert N. Ling, "A Physical Theory of the Living State (Waltham, Massachusetts: Blaisdell Publishing Company, A Division of Ginn and Company, 1962) p. 75.

4. *The Equation for Solute Distribution in Living Cells According to the Association–Induction Hypothesis*

Figure 9 shows a diagram of a portion of a living cell in contact with its external medium. Within the cell ions exist in two states, free and adsorbed. The model cell shown possesses three types of protein sites which adsorb alkali-metal cations. Two of these types of sites prefer K^+ ion over Na^+ ion; one prefers Na^+ ion over K^+ ion. Based on this model, the concentrations of the intracellular ions can be expressed by the following equations:

$$[Na^+]_{in} = \alpha[Na^+]_{int} + [Na^+]^{I}_{ad} + [Na^+]^{II}_{ad} + [Na^+]^{III}_{ad} \qquad (1)$$

and

$$[K^+]_{in} = \alpha[K^+]_{int} + [K^+]^{I}_{ad} + [K^+]^{II}_{ad} + [K^+]^{III}_{ad} \qquad (2)$$

where $[Na^+]_{in}$ and $[K^+]_{in}$ are the total intracellular concentrations of Na^+ ion and K^+ ion, respectively, α is the percentage of water in the cell. $[Na^+]_{int}$ and $[K^+]_{int}$ are the concentrations of interstitial K^+ and Na^+ ion, respectively. $[Na^+]^{I}_{ad}$ and $[K^+]^{I}_{ad}$ are adsorbed Na^+ and K^+ ion on the type I sites, $[Na^+]^{II}_{ad}$ and $[K^+]^{II}_{ad}$ on the type II sites, and so forth. Intracellular and

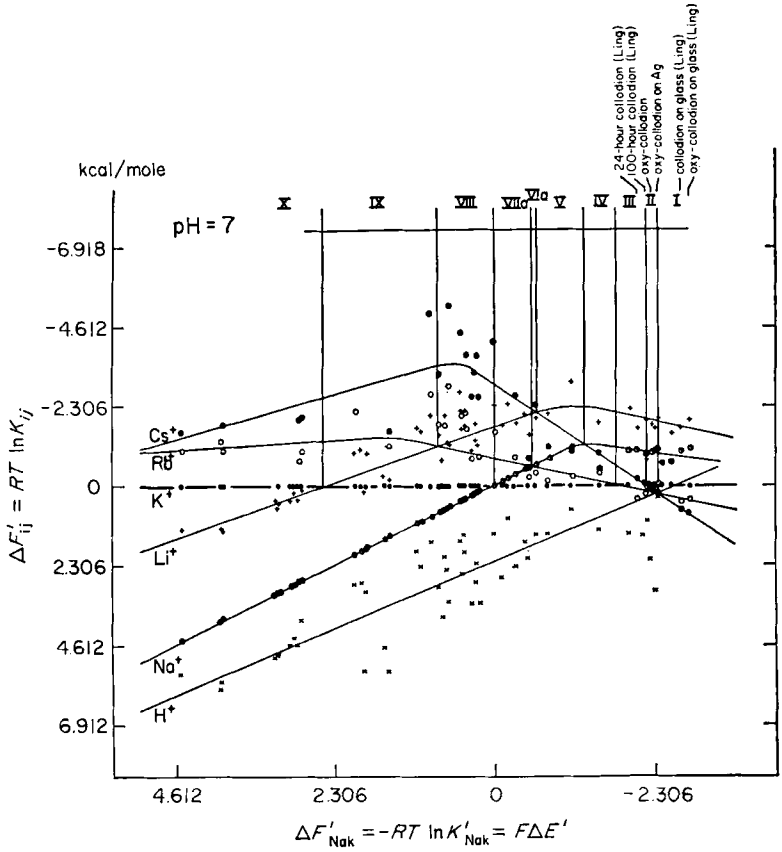

FIG. 8. Ionic specificity in ionic glass electrode potentials at neutral pH. Each vertical row of data points corresponds to the observed selectivity properties of a particular material (Eisenman, 1961).

adsorbed ion concentrations are in units of moles per kilogram of fresh cells. Interstitial ion, on the other hand, is in moles per liter of cell water. Putting Eqs. (1) and (2) in a more general form:

$$[Na^+]_{in} = \alpha[Na^+]_{int} + \sum_{L=1}^{N} [Na^+]^{L}_{ad} \qquad (3)$$

and

$$[K^+]_{in} = \alpha[K^+]_{int} + \sum_{L=1}^{N} [K^+]_{ad}^{L} \tag{4}$$

Here $[Na^+]_{ad}^{L}$ and $[K^+]_{ad}^{L}$ refer to the concentrations of adsorbed Na+ and K+ ion on the Lth type of sites. In the case shown in the diagram of Fig. 9, there are a total of three types of sites, therefore $N = 3$.

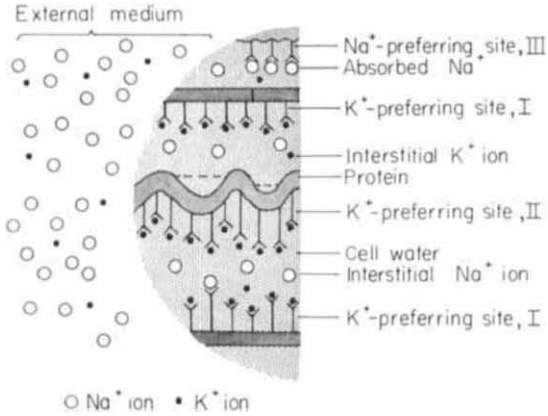

FIG. 9. Diagrammatic illustrations of a living cell. Stipled area represents space filled with water in polarized multilayers.

a. The Equation for the Interstitial Ion. Let us first consider the distribution of interstitial ions. According to Henry's law, the ratio of the concentrations of a solute distributed between two solvents at equilibrium with each other is a constant over a considerable concentration range (see also Troschin, 1958). Thus, in the case of the distribution of Na+ ion between the cell water and the external aqueous medium, the ratio of internal to external Na+ ion concentrations is a constant q_{Na} called the distribution coefficient. Thus

$$\frac{[Na^+]_{int}}{[Na^+]_{ex}} = q_{Na} \tag{5}$$

where $[Na^+]_{ex}$ is the external Na+-ion concentration. Similarly

$$\frac{[K^+]_{int}}{[K^+]_{ex}} = q_K \tag{6}$$

where $[K^+]_{ex}$ is the external K+-ion concentration and q_K is the equilibrium distribution coefficient of K+ ion. Rearranging Eqs. (5) and (6):

$$[Na^+]_{int} = q_{Na}\,[Na^+]_{ex} \tag{7}$$

and

$$[K^+]_{int} = q_K [K^+]_{ex} \tag{8}$$

According to these equations, a plot of the interstitial Na^+- (or K^+-) ion concentration as a function of the external Na^+- (or K^+-) ion concentrations should yield a straight line having a slope equal to q_{Na} (or q_K). Further, there is no competition among ions in the interstitial water, i.e., the same concentration of Na^+ ion is found in the cell water whether or not K^+ ion is also present.

b. The Equation for the Adsorbed Ions. If the concentration of the type I adsorption sites shown in Fig. 9 is $[f]^I$ and if each site can be occupied by one ion at a time, the total number of Na^+ ions adsorbed on the type I sites can be described by the Langmuir adsorption isotherm (Langmuir, 1917).

$$[Na^+]^I_{ad} = \frac{[f]^I \tilde{K}^I_{Na} [Na^+]_{ex}}{1 + \tilde{K}^I_{Na} [Na^+]_{ex} + \tilde{K}^I_K [K^+]_{ex}} \tag{9}$$

where K^I_{Na} and K^I_K are the adsorption constants of Na^+ and K^+ ion, respectively, on this type of site in M^{-1}. Similarly, for K^+-ion adsorption on type I sites:

$$[K^+]_{ad} = \frac{[f]^I \tilde{K}^I_K [K^+]_{ex}}{1 + \tilde{K}^I_{Na} [Na^+]_{ex} + \tilde{K}^I_K [K^+]_{ex}} \tag{10}$$

A plot of $[Na^+]_{ad}$ against $[Na^+]_{ex}$ is a hyperbola (see, for example Figs. 26 and 30): That is, at low $[Na^+]_{ex}$ values the sites are largely empty and there is a proportionate increase of adsorbed Na^+ ion with increasing $[Na^+]_{ex}$. At higher $[Na^+]_{ex}$, the sites become more and more occupied. The increment of adsorbed Na^+ ion with a unit increment in $[Na^+]_{ex}$ diminishes steadily until the total adsorbed Na^+ ion approaches a maximum value equal to the total number of sites, $[f]^I$. Equation 9 shows that the adsorbed Na^+ ion can be decreased by increasing the concentration of the competing K^+ ion. At a sufficiently high K^+-ion concentration, the adsorbed Na^+ ion can be reduced to an insignificant level.

Equation 9 can be written in reciprocal form:

$$\frac{1}{[Na^+]_{ad}} = \frac{1}{[f]^I \tilde{K}^I_{Na}} (1 + \tilde{K}^I_K [K^+]_{ex}) \frac{1}{[Na^+]_{ex}} + \frac{1}{[f]^I} \tag{11}$$

If one plots $1/[Na^+]_{ad}$ as a function of $1/[Na^+]_{ex}$ at constant $[K^+]_{ex}$, one obtains a straight line. The intercept on the ordinate (i.e., at $1/[Na^+]_{ex} = 0$) is the reciprocal of the total concentration of type I sites. The slope of the lines is a function of $[K^+]_{ex}$, $\tilde{K}^I_K$, and $\tilde{K}^I_{Na}$. The reciprocal form of Eq. (10) for K^+-ion adsorption is

$$\frac{1}{[K^+]^I_{ad}} = \frac{1}{[f]^I \tilde{K}^I_K}(1 + \tilde{K}^I_{Na}[Na^+]_{ex})\frac{1}{[K^+]_{ex}} + \frac{1}{[f]^I} \quad (12)$$

If Eqs. (7) and (9) are substituted into Eq. (3) and Eqs. (8) and (10) are substituted into Eq. (4), one obtains the explicit equations for the total Na^+- and K^+-ion concentrations in living cells.

$$[Na^+]_{in} = \alpha q_{Na}[Na^+]_{ex} + \sum_{L=1}^{N} \frac{[f]^L \tilde{K}^L_{Na}[Na^+]_{ex}}{1 + \tilde{K}^L_{Na}[Na^+]_{ex} + \tilde{K}^L_K[K^+]_{ex}} \quad (13)$$

and

$$[K^+]_{in} = \alpha q_K[K^+]_{ex} + \sum_{L=1}^{N} \frac{[f]^L \tilde{K}^L_K[K^+]_{ex}}{1 + \tilde{K}^L_{Na}[Na^+]_{ex} + \tilde{K}^L_K[K^+]_{ex}} \quad (14)$$

Here $\tilde{K}^L_{Na}$ and $\tilde{K}^L_K$ are the adsorption constants of Na^+ and K^+ ion on the Lth adsorption site. Eqs. (13) and (14) are basically similar to an equation first introduced by Troschin for sugar distribution in cells (Troschin, 1958). They will be henceforth referred to as the Troschin equations.

B. The Molecular Mechanism for Solute Distribution in Living Cells: Experimental Evidence

1. The Physical State of Water in Living Cells and Model Systems

The adsorption of molecules in polarized multilayers on solid surfaces is described by an equation of Bradley (Bradley, 1936; see also de Boer and Zwikker, 1929)

$$\log_{10}\frac{p_0}{p} = K_1 K_3{}^a + K_4 \quad (15)$$

where a is the amount of gas (water in the present case) adsorbed, at vapor pressure p; p_0 is the vapor pressure at saturation. K_1, K_3 and K_4 are constants. As Fig. 10 shows, this equation is followed by the sorption of water onto an isolated protein, sheep's wool (Ling, 1965c). The entire range of experimental data from Bull (1944) fit Eq. (15). Similar results are obtained for the sorption of water onto collagen (Ling, 1965c) and other proteins and macromolecules (Mellon and Hoover, 1950).

These experiments indicate that proteins, *in vitro,* have the capability of organizing the water with which they are in contact into polarized multilayers. One would expect that cellular proteins, *in vivo,* would have the same property and, indeed, there are two lines of evidence indicating that the water in cells *is* in a different state from the water in a dilute salt solution.

i. Intracellular freezing pattern. Normal water or a dilute salt solution, when cooled to below 0°C., forms tridymite ice in hexagonal patterns (Hallett, 1965). In overall shape, normal ice is featherlike with branches at regular intervals (Fig. 11). Ice formed in supercooled living cells by seeding with an ice-tipped micropipette is abnormal in structure (Chambers and Hale, 1932; Rapatz and

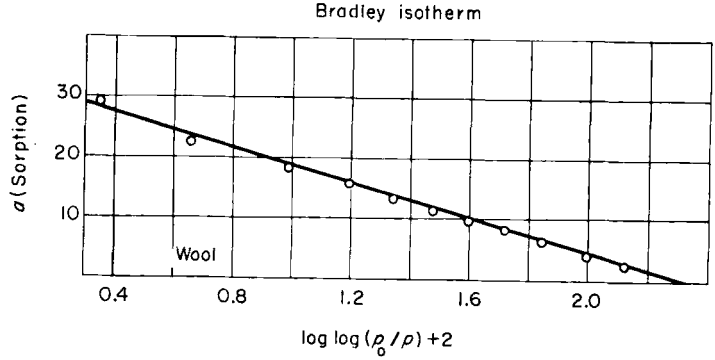

FIG 10. Sorption of water vapor on sheep's wool, plotted according to the Bradley multilayer adsorption isotherm. Data of Bull (1944) (Ling, 1966a, by permission of *Annals of the New York Academy of Sciences*).

Luyet, 1958). In skeletal muscle, for example, longitudinal spikes following the direction of muscle protein filaments are formed (Chambers and Hale, 1932; Rapatz and Luyet, 1958) (Fig. 12). Such spikes, which have no branches, indicate that the intracellular water is not normal. That this abnormality is intimately associated with the structure and orientation of the cell proteins (Ling, 1965a, 1966b, 1967a) is indicated by the demonstration that when the myofilaments are twisted, the spikes also become twisted (Chambers and Hale, 1932).

ii. Nuclear magnetic resonance (NMR). The recently developed technique of nuclear magnetic resonance spectroscopy is being used with increasing effectiveness to study the physical state of water in cells. From the widening of the NMR signal of the water in rabbit sciatic nerve and its dependence on the orientation of the magnetic field, Chapman and McLauchlen concluded that the bulk of this intracellular water is not normal but is in a partially oriented state (Chapman and McLauchlan, 1967) (Fig. 13). Fritz and Swift (1967) reached a similar conclusion working with frog nerves. [For criticism of the earlier conclusion of Bratton *et al.* (1965) that only part of the muscle cell water suffers restricted rotation, also see Fritz and Swift (1967)].

2. *Ionic Exclusion from the Water of Sheep's Wool, Frog Muscle, and in Actomyosin Gel*

Figure 14 shows the equilibrium ionic uptake of sheep's wool. In the presence of high concentrations of a competing ion, a plot of the accumulated labeled

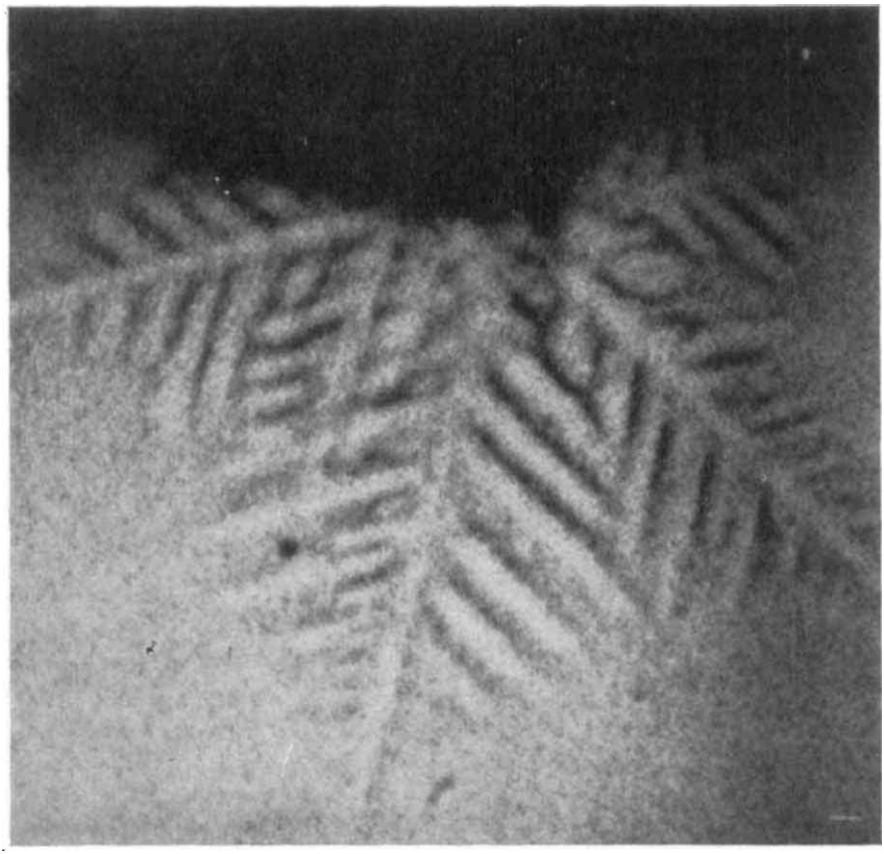

FIG. 11. Ice crystal growth in supercooled pure water initiated by the insertion of a single crystal at —3.5°C. (Hallett, 1965, by permission of *Federation Proceedings*).

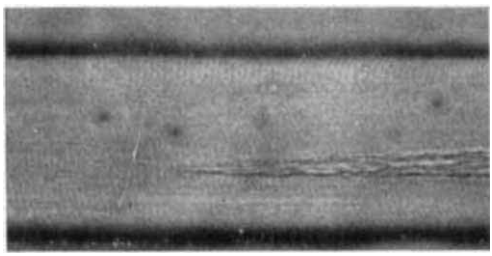

FIG. 12. Development of an ice spear in a single muscle fiber at —2.5° C. (Rapatz and Luyet, 1958, by permission of *Biodynamica*).

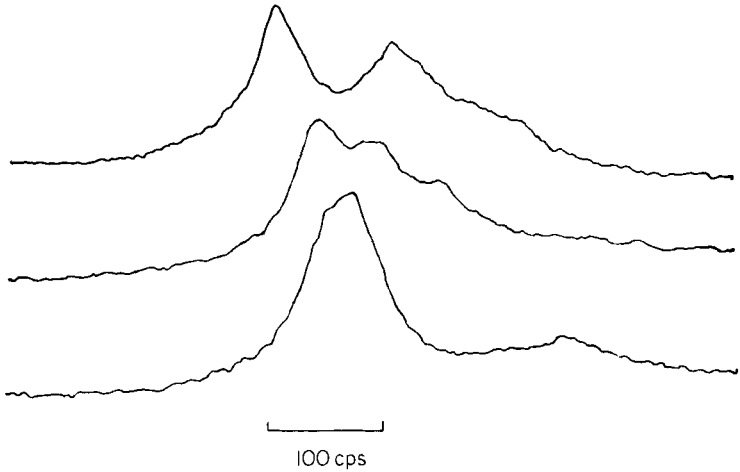

FIG. 13. NMR spectra of water in rabbit sciatic nerve: (top) with nerve axis parallel to the applied field; (center) axis perpendicular to the field: (bottom) nerve axis at approximately 54° to the direction of the applied field (Chapman and McLauchlan, 1967, by permission of *Nature*).

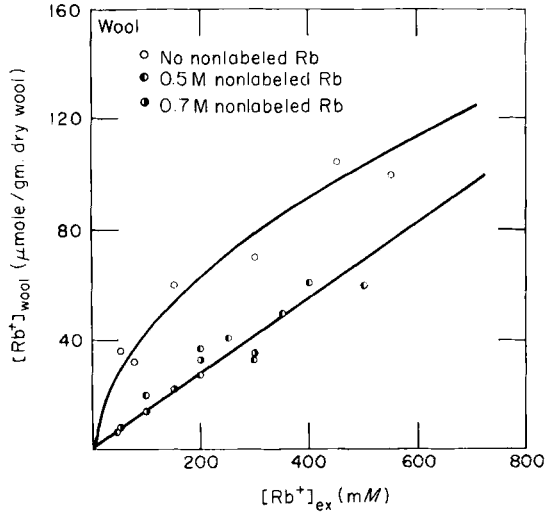

FIG. 14. Equilibrium labeled Rb+-ion distribution in sheep's wool in the presence of varying concentrations of competing nonlabeled Rb+ ion. Increasing the nonlabeled Rb+-ion concentration from 0 to 0.5 *M* reduced the labeled Rb+ concentration. Further increase from 0.5 to 0.7 *M*, however, produced no further decrease of the labeled Rb+-ion concentration in the wool and the distribution curve is linear. The wool contains 30% water. Assuming all labeled Rb+ ion in the presence of 0.5 or 0.7 *M* nonlabeled Rb+ ion to be in this water, the distribution coefficient of the labeled Rb+ ion is about 0.29.

Rb+ ion as a function of the external Rb+-ion concentration approaches a straight line (lower line). In the absence of competing ion, there is an additional fraction of Rb+ ion in the wool which is not linearly related to the external Rb+-ion concentration. In fact, subtracting the lower curve from the upper curve gives a hyperbola. These data indicate that ionic accumulation in sheep's wool follows an equation similar to Eq. (13) or (14) (Ling, 1965b).

Considering only the linear fraction, we note that the slope of this line is only 0.12, indicating that in this system which constitutes 30% protein and 70% water, Rb+ ion is accommodated to only 29% of its concentration in the external solution. Thus, the effect of the polarization of the water into multilayers as described above is the partial exclusion of solutes from this water.

Figure 15 shows the equilibrium Na+-ion uptake of living frog sartorius

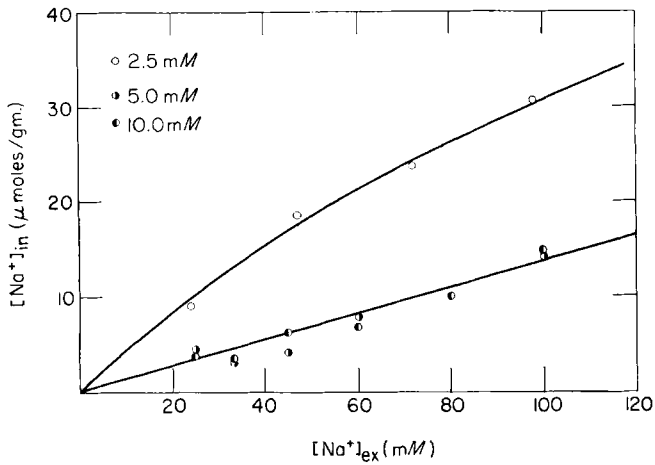

FIG. 15. Equilibrium distribution of Na+ ion in frog sartorius muscle in the presence of varying external K+-ion concentrations. The external K+-ion concentrations are 2.5 m*M*, 5.0 m*M*, and 10.0 m*M*. The data were calculated on the basis of a 10% extracellular space. The slope of the straight line going through the points at the higher K+-ion concentrations is 0.14. The muscle cells contain 78% water. If all Na+ ion in the cell at the higher K+-ion concentrations is assumed to be in the cell water, the equilibrium distribution coefficient of Na+ ion between the cell water and the external medium is 0.18.

muscle (Ling, 1965a,b, 1966b; Troschin, 1958). As in sheep's wool, increasing the concentration of competing K+ ion lowers the intracellular Na+-ion concentration. Again, however, the intracellular Na+-ion concentration is not reduced to zero at high K+ ion. Instead, there is a level beyond which no further increase of K+-ion concentration has any effect on the Na+ ion in the cell. This remaining fraction (B) of intracellular Na+-ion concentration is also linearly related to the external Na+-ion concentration with a slope of about 0.14. As in the case of

sheep's wool, at lower concentrations of competing K+ ion, there is an additional fraction of Na+ ion (A fraction) which is roughly hyperbolic in its relation to the external Na+-ion concentration (see Section III, D,10).

Figure 16 shows the equilibrium Rb+-ion distribution in a protein–water

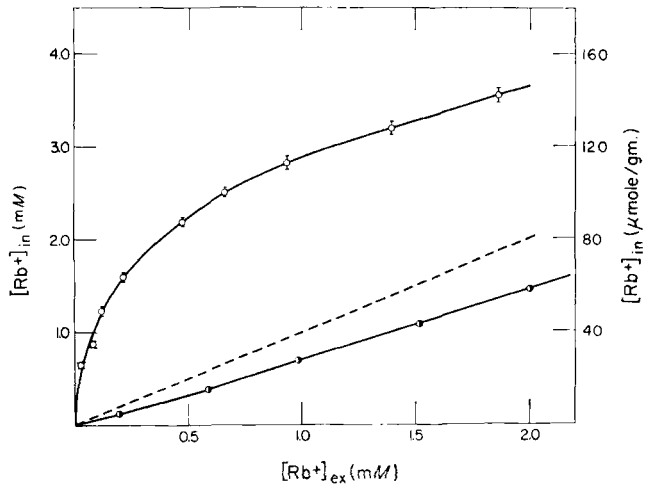

FIG. 16. The equilibrium distribution of labeled Rb+ ion in isolated actomyosin gel at neutral (6.7) and acidic pH (4.3).

system (actomyosin) taken from the living cell (Ling and Ochsenfeld, 1968a). Here the Rb+-ion distribution follows the same pattern as seen in sheep's wool and in living muscle. In the presence of a strongly competing cation (H+ ion, pH 4.4), the concentration of Rb+ ion in the gel is linearly related to the external Rb+-ion concentration (B fraction). At lower H+-ion concentration, an additional fraction (A), having the typical characteristics of a Langmuir adsorption isotherm, is superimposed on the B fraction. The actomyosin gel is perfectly homogeneous and contains no anatomical structures, yet the Rb+-ion concentration in the gel water at low pH is only a fraction (50–70%) of that of the external solution.

From these data we reach the conclusion that the water in this gel again has abnormal solubilities for alkali-metal ions. The actomyosin gel used in the investigation shown in Fig. 16 is very dilute (3–5% protein versus 95–97% water). Together with other proteins, actomyosin exists as a much more concentrated gel in the living muscle (20% protein versus 80% water). The ion-exclusion property of the water of isolated actomyosin gel is a compelling reason to believe that the ions of the B fraction of Na+ ion in frog muscle (Fig. 15) represent the fraction in the muscle cell water and that the water in muscle

cells similar to that in sheep's wool accommodates less alkali-metal ion than the external aqueous solution.

3. The Entropic Basis of Ion Exclusion from the Water in Actomyosin Gel

Ling and Ochsenfeld studied the temperature coefficient of the exclusion of Rb^+ and other alkali-metal ions from the water in isolated actomyosin gel (Ling and Ochsenfeld, 1968a). From these studies, the conclusion was drawn that the exclusion was primarily attributable to the unfavorable entropy of the hydrated alkali-metal ion in the gel water.[4]

4. The Adsorbed Fraction of Na^+ Ion

We have shown above (Fig. 15) that increasing the K^+-ion concentration to a certain level brings about a reduction in the level of intracellular Na^+ ion in frog sartorius muscle. This suggests that the K^+ ion is competing with an adsorbed fraction of Na^+ ion. There is now considerable independent evidence that such a fraction does indeed exist: (1) Lewis and Saroff (1957) showed Na^+ ion binding onto isolated actomyosin. (2) Hinke (1959) used an intracellular Na^+-ion-sensitive microelectrode to study the activity of Na^+ ion in frog muscle and squid axon and concluded that about two-thirds of the intracellular Na^+ ion is bound.[5] (3) Recently Cope (1967) has used the techniques of NMR to study the Na^+ ion in muscle and has concluded that about 70% of this ion is complexed. A similar conclusion was reached by Rotunno *et al.* (1967) in regard to Na^+ ion in frog skin cells. Thus, under normal conditions the intracellular Na^+ ion is made up of an adsorbed fraction as well as the interstitial fraction discussed above.

5. K^+-Ion Accumulation

a. Interpretation According to the Association-Induction Hypothesis. In Fig. 17 the reciprocal of the intracellular labeled K^+-ion concentration is plotted as a function of the reciprocal of the external labeled K^+-ion concentration.

Varying the external nonlabeled K^+-ion concentration produces a family of straight lines converging at the same locus on the ordinate. Such a plot is characteristic of a Langmuir adsorption isotherm [Eq. (11)] and in terms of the association–induction hypothesis indicates that the intracellular K^+ ion is all in

[4] *Note Added in Proof:* Recently Gary-Bobo and Solomon [Gary-Bobo, C. M. and Solomon, A. K. (1968). *J. Gen. Physiol.* **52**, 825] published results of their studies on the distribution of K^+ ion in hemoglobin solutions. At low pH, an exclusion of K^+ ion from this protein solution was also observed and was attributed by these authors to a Donnan effect. Whether this is a better explanation applicable to our *in vitro* actomyosin data (or vice versa) remains to be determined.

[5] *Note Added to Proof:* For comments on the use of ion-sensitive electrode to assay ionic activity in living cells see Ling [Ling, G. (1969). *Nature* **221**, 386].

the adsorbed state. The concentration of K^+ ion is many times higher in the muscle cell (90 mM) than in the frog plasma (2.5 mM). Thus the interstitial K^+ ion can amount to only a fraction of the concentration in the external solution and hence less than 1–2% which is the limit of experimental error. From

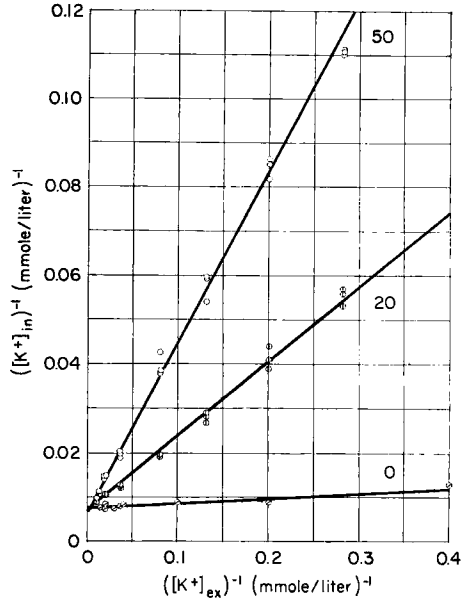

FIG. 17. Intracellular labeled K^+-ion concentration plotted reciprocally against the external labeled K^+-ion concentration, with which it is in equilibrium, in the presence of 0, 20, and 50 mmole/liter of nonlabeled potassium acetate. Labeled K^+ was also in the form of acetate salt. Each point represents the labeled K^+-ion concentration in a single frog sartorius muscle; lines obtained by the method of least squares. On the lowest curve within the area from $[K^+]_{ex}^{-1} = 0$ to 0.05 (mmole/liter)$^{-1}$ and from $[K^+]_{in}^{-1} = 0$ to 0.01 (mmole/kg.)$^{-1}$, a total of 23 points was determined; they fall so close to one another that only a few could be represented. All the others would be superimposed on these. Data from two series of experiments (Ling and Ochsenfeld, 1966, by permission of *The Journal of General Physiology*).

these data we obtain an association constant for K^+ ion of 665 M^{-1} and a concentration of anionic sites $[f]$ equal to 143 mmoles per kilogram fresh cells. From the known protein content of muscle and the percentage of acidic side chains on these proteins the maximum number of anionic sites in the cell is 260 mmoles/kg. which is more than enough to account for this number of K^+-ion adsorbing sites (Ling and Ochsenfeld, 1966).[6]

[6] *Note Added in Proof:* For additional NMR evidence that the bulk of intracellular K^+ ion is in an adsorbed state see Ling and Cope [Ling, G. N., and Cope, F. W., *Science* **163**, 1335 (1969)].

b. Alternative Interpretations. i. Donnan equilibrium. While competition is usually considered a distinguishing feature of the Langmuir adsorption isotherm, it may also follow from the fact that in a Donnan equilibrium macroscopic electroneutrality must be maintained (Ling and Ochsenfeld, 1966). However, a Donnan system can be differentiated from a system in which the K^+ ion is adsorbed by studying the effect of a second ion on the equilibrium distribution of labeled K^+ ion and comparing the effect of this second ion with that of nonlabeled K^+ ion. In the case of a Donnan equilibrium, the difference between the two effects depends on the difference between the respective activity coefficients. In Fig. 18 we have compared the effect of similar concentrations of Cs^+ ion and nonlabeled K^+ ion on the equilibrium accumulation of K^+ ion. The experimentally observed difference is far larger than can possibly be accounted for by the difference in the activity coefficients (less than 2%).

ii. The carrier model. According to a recent version of the membrane theory, the majority of K^+ ion enter the cell by combining with certain hypothetical "carrier" molecules which then ferry the K^+ ion across the lipid part of the plasma membrane (Osterhout, 1936; Jacques, 1936; Epstein and Hagen, 1952). Once the carrier-K^+-ion complex reaches the inner surface of the cell membrane, the K^+ ion dissociates, entering the cell water. This idea is similar to Overton's postulation, at the turn of the twentieth century, of adenoid or secretary activity. The best evidence that can be cited in favor of such a carrier hypothesis comes from studies of the initial rate of entry of K^+ ion. Thus this rate of entry shows saturability (i.e., as the external K^+ ion increases, the rate of entry per unit increment of external K^+-ion concentration steadily decreases to approach zero) and competition (i.e., similar alkali-metal ions compete with K^+ ion and reduce its rate of entry) (Fig. 19; Ling and Ochsenfeld, 1965).

Fundamental difficulties of the carrier model. (1) Historically the entry of K^+ ion was always considered to involve diffusion of the free ion through the cell membrane. Bernstein's original version of the membrane theory (Bernstein, 1902) of the resting potential was based on this proposition. Postulation of the Na^+ pump did not involve a revision of this concept. Thus the Hodgkin–Katz–Goldman equation [Eq. (16)] was derived on the basis that K^+ ion migrates through the cell membrane as a postively charged ion under the influence of the constant electric field. If the K^+ ion traverses the cell membrane in combination with a carrier, there are two possibilities: Either the carrier molecule bears an anionic charge, or it is a neutral molecule. If K^+ ion combines with a carrier bearing a negative charge, the foundation of the Hodgkin–Katz–Goldman equation is removed: The constant electric field would have no effect on the direction of motion of a neutral complex.

If, on the other hand, one considers the carrier itself to be uncharged, the carrier-K^+-ion complex would be a monovalent cation. This would overcome the above-mentioned difficulty. Another difficulty now arises, however, because of

the enormous gain of free energy when a charged ion is brought into a lipid phase. To achieve this, the carrier must possess both a strong affinity for K+ ion and qualities that allow itself to stay permanently in the lipid membrane. It is

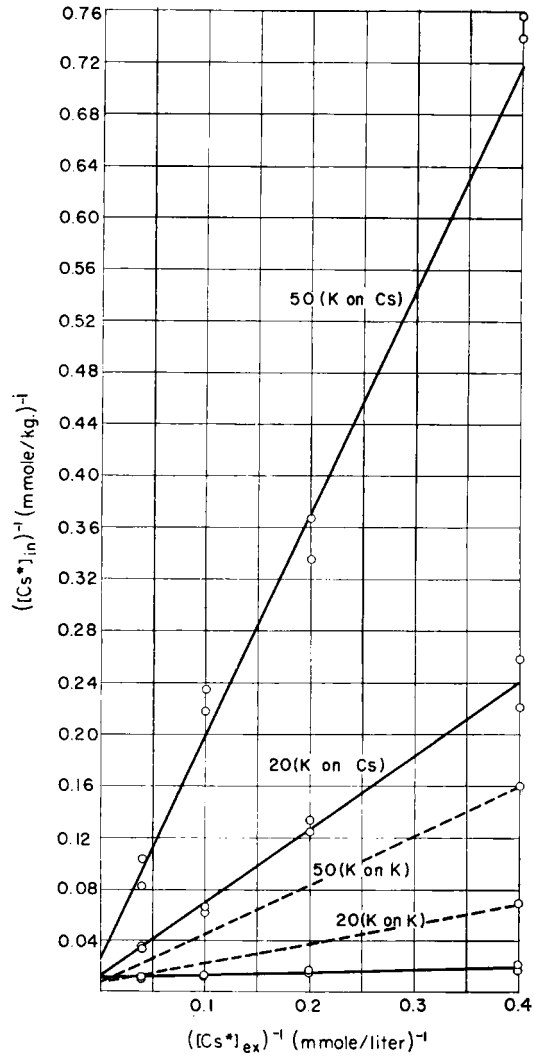

FIG. 18. Equilibrium labeled Cs+-ion concentration in muscle cells plotted reciprocally against the external Cs+-ion concentration with which it is in equilibrium. Competing K+-ion concentrations are 0, 20, and 50 mmole/liter respectively. Both Cs+ and K+ were in the form of acetates (24°C.). Each point represents a single determination on one frog sartorius muscle; lines obtained by the method of least squares. The effect of K+ ion on the accumulation of labeled K+ ion (dotted lines) taken from Fig. 1 for comparison (Ling and Ochsenfeld, 1966, by permission of *The Journal of General Physiology*).

not easy to construct a molecule with these conflicting attributes. Perhaps this is why, in spite of the long history of the carrier, there is no experimental model that demonstrates the behavior observed, e.g., saturability and competition.

It hardly needs to be pointed out that saturability and competition are evidence only that entry is associated with a limited number of sites. Thus, the rate of entry of K^+ ion into a sheet of ion-exchange resin shows entirely similar saturability and competition (Ling and Ochsenfeld, 1965) (see also Fig. 20). Here such a resin is nothing but a three-dimensional anion-bearing matrix possessing neither carriers nor membranes. Recently, Ling and Ochsenfeld have succeeded in demonstrating similar saturability and competition in the rate of entry of Rb^+ ion into layers of an isolated cytoplasmic protein–water system (actomyosin gel). In such a system the rate of entry is not surface- but bulk-phase-limited (Ling and Ochsenfeld, 1968b). This data shows that even in the absence of a cell membrane, ion entry follows the kind of kinetics shown in Fig. 19. Thus saturability and competition result from the presence of a limited number of adsorption sites throughout the entire protein–water system.

(2) Figure 21 shows the reciprocal of the initial rate of entry of Na^+ ion plotted as a function of the reciprocal of the external Na^+ ion concentration in the presence of varying concentrations of K^+ ion. Although there is a fraction of Na^+ ion entry whose rate is decreased by increasing the K^+-ion concentration

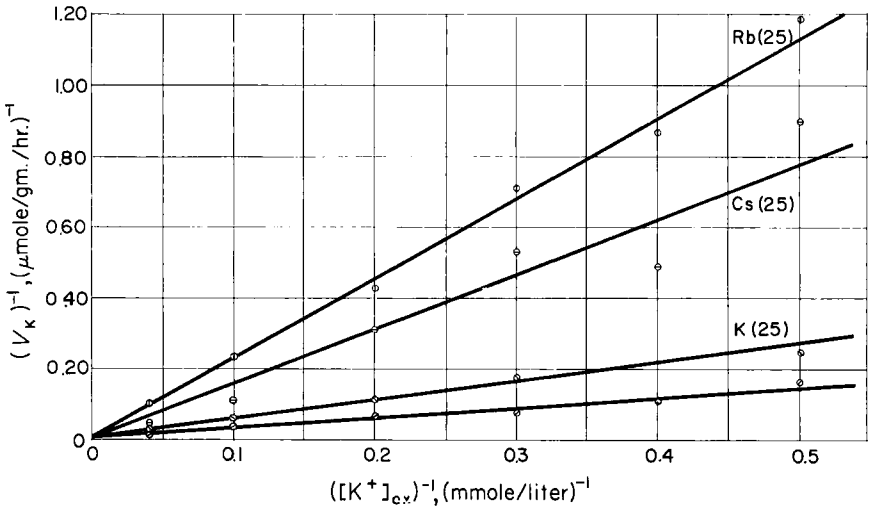

FIG. 19. Inhibitory effect of 25 mmole/liter of Rb^+, Cs^+, and nonlabeled K^+ ion on the initial rate of entry of labeled K^+ ion into frog sartorius muscles. Lowest, nonlabeled curve represents the rate of K^+-ion entry with no added competing ion. Muscles were soaked for 30 minutes at 24°C., followed by 10 minutes of washing at 0°C. Each point represents a single determination on two sartorius muscles (Ling and Ochsenfeld, 1965, by permission of *Biophysical Journal*).

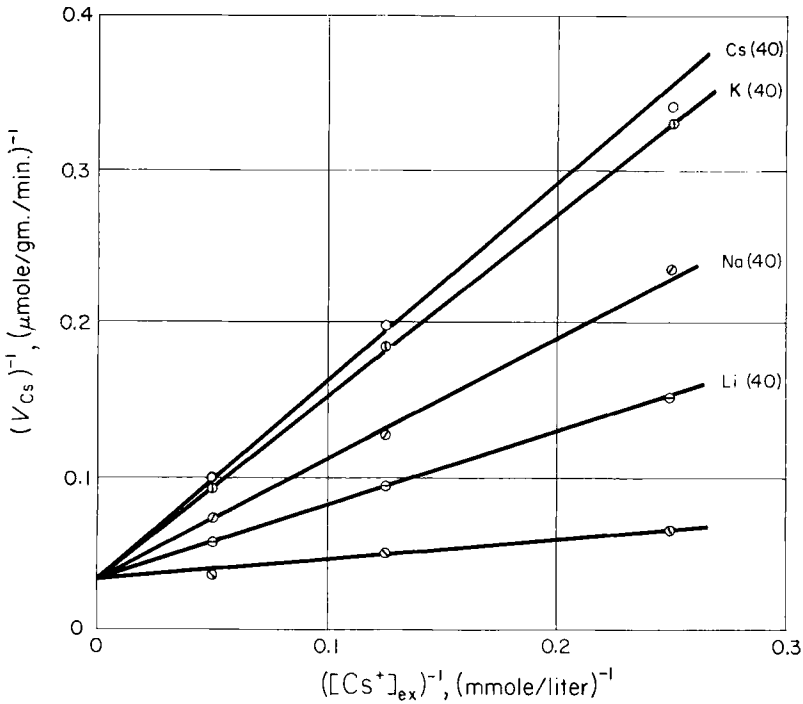

FIG. 20. Effects of CsCl, KCl, NaCl, and LiCl on the initial rate of entry of labeled Cs+ ion into ion-exchange resin sheets. Nalfilm-1 strips soaked for 2 minutes at 5°C. in an experimental solution containing (approximately) 2.5 mmole tris buffer at pH 7.0, the labeled entrant ion and nonlabeled ion (40 mmole/liter) as indicated in the figure. Strips washed for 10 seconds in cold distilled water (0°C.) before counting (Ling and Ochsenfeld, 1965, by permission of *Biophysical Journal*).

from 0 to 30 m*M*; another fraction, shown by the upper line, is unaffected by K^+-ion concentrations as high as 100 m*M*. This upper line goes through the origin indicating that there is no saturation in the entry of this fraction (i.e., an inflnite number of "adsorption sites"). Thus there is a fraction of Na^+ ion which shows neither competition nor saturation and thus cannot be conceived to enter via carriers, but must enter via aqueous channels. If such aqueous channels, large enough for the hydrated Na^+ ion, exist, it is hard to understand how they could exclude the smaller hydrated K^+ ion.

C. Answers to Fundamental Criticisms of Ionic Adsorption in Living Cells

There are a number of lines of experimental evidence that seem, superficially at least, to contradict the adsorption model for ionic accumulation in living cells. Let us describe this evidence first and then discuss some recent advances in our understanding of adsorption that serve to change this picture.

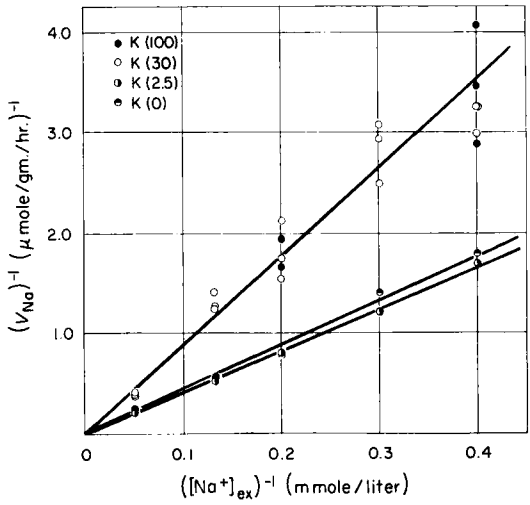

FIG. 21. Effect of various concentrations of K+ ion on the initial rate of entry of Na+ ion into frog sartorius muscles. Increasing the K+-ion concentration from 30 mmole/liter to 100 mmole/liter causes no apparent effect on the rate of Na+-ion entry, while reduction from 30 mmole/liter to 2.5 mmole/liter causes an increased rate of Na+-ion entry. Fifteen minutes of soaking at 25°C. were followed by washing for 10 minutes at 0°. Each point represents average of three individual determinations (Ling and Ochsenfeld, 1965, by permission of *Biophysical Journal*).

(1) Living cells are isotonic with an approximately 0.1 *M* aqueous NaCl solution. This demands that the osmotic activity within the cells be equal to that of this solution. Since the total ionic concentration in the cell is approximately 0.1 *M* and K+ ion constitutes the bulk of the cations, it follows that all or nearly all of this K+ ion as well as the intracellular anions must be in a free state such as is found in 0.1 *M* NaCl (Hill, 1930).

(2) If a pair of electrodes are placed on the surface of an intact nerve or muscle fiber, the total resistance measured is, relatively speaking, little affected by the distance between the electrodes. This was interpreted as being the result of high membrane resistance and low cytoplasmic resistance (the core-conductor theory of Hermann (Hermann, 1879). The low cytoplasmic resistance was interpreted as indicating complete or nearly complete dissociation of the intracellular K+ ion.

(3) The mobility of labeled K+ ion in squid axons averages 1.5×10^{-5} cm.^{2}/sec. This value is not too far from the diffusion coefficient of K+ ion in an aqueous KCl solution of a concentration comparable to that of squid cytoplasm (2.14×10^{-5} cm.^{2}/sec.). Thus, the conclusion was drawn that the bulk of K+ ion inside an axon exists as free ions (Hodgkin and Keynes, 1953).

(4) Bernstein's membrane theory of cellular electrical potential (Bernstein, 1902) and its modified version introduced by Hodgkin and Katz (Hodgkin and Katz, 1949) predicts the correct magnitude of the resting potential. Since this theory is based on the assumption of complete dissociation of intracellular K^+ ion, it follows that the bulk of the intracellular K^+ ion must be in the free state.

Considered together, this evidence is too compelling to ignore. It is not surprising that many cell biologists have so far considered the membrane theory a better choice. However, with a fuller understanding of both the state of water in living cells and the nature of adsorption, it becomes possible to resolve the conflict. In the following discussion, we will note point-by-point answers to the criticisms listed above.

(1) The postulate that the bulk of the intracellular ions must be free in order that the cell be iso-osmotic with a 0.1 *M* NaCl solution is valid only in so far as there is no interaction between the cell water and the cell proteins as postulated by the membrane theory (see above). There is now overwhelming evidence that the bulk of the water in the cell is adsorbed as polarized multilayers on the proteins. Thus the lowering of the activity of water within the cell (expressed as osmotic pressure) is explained by the interaction of water with the proteins. With this degree of interaction with and lowering of water activity by proteins, the fact that the total osmotic pressure does not exceed that of a 0.1 *M* NaCl solution, suggests intracellular ionic adsorption.

Arguments (2) and (3) can be answered together. It is well known that in nerve and muscle cells the major protein components are oriented in a longitudinal direction (Chambers and Kao, 1952; Huxley, 1957). Thus one might anticipate a longitudinal orientation of the anionic sites as shown diagrammatically in Fig. 22. In this diagram concentric circles surrounding each anionic site represent equipotential lines. The closer they are to the anionic site, the lower the potential. As the diagram shows, these lines overlap. In seeking a minimum energy path, an adsorbed K^+ ion on one site can, therefore, pass from one site to another by following the overlapping regions of low energy. The activation energy for this migration is therefore low. Thus one may say that by a sequential orderly arrangement of anionic sites, a "conduction band" is provided for the K^+ ion (for further details, see Ling, 1962, Chap. 11). On the other hand, the distance between the myofilaments is such that a greater distance separates sites on neighboring protein chains. In consequence, a much higher activation energy has to be overcome before a radial migration of the K^+ ion can be achieved. If this hypothesis is correct, we might anticipate the longitudinal migration of K^+ ion in the cell to be equal to and perhaps even faster than K^+-ion migration in a dilute salt solution. On the other hand, radial migration of K^+ ion would be slow. This can then explain both the core conduction behavior of muscle and nerve cells and the longitudinal K^+-ion mobilities in squid axons. Two lines of in-

dependent experimental evidence suggest that this explanation is the proper one: (a) It has been known for a long time that K^+-ion migration on the surface of glass that bears anionic sites is faster than K^+-ion migration in dilute solution (McBain and Peaker, 1930; Mysels and McBain, 1948; Nielsen *et al.*, 1952). (b) Schwindewolf (1953) and Heckmann (1953) have shown that the elec-

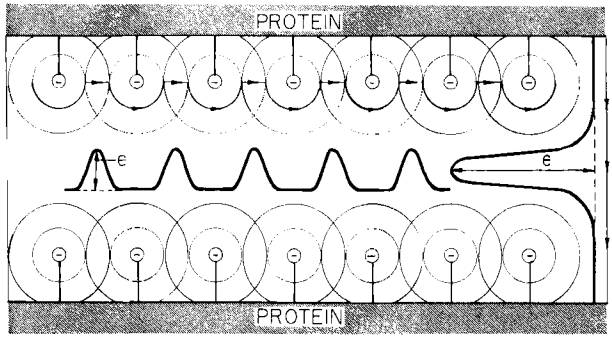

FIG. 22. Diagrammatic illustration of an effective "conduction band" for adsorbed ions along a longitudinal array of anionic sites. Transversely, the anionic sites are too far apart to produce a conduction band and low conductance results. The concentric circles represent equipotential lines with lower potentials closer to the anions. The line with the arrows indicates a probable path for an adsorbed ion moving along the "conduction band"; it has to overcome relatively low activation energies because of the overlapping of the electric fields. Much larger activation energy has to be overcome for transverse migration.

trical conductance of a solution containing linear anionic polymers (i.e., polyphosphate, thymonucleic acid, or solubilized silk protein) and flowing in a long tube is anisotropic. That is, the conductance is higher in the direction parallel to the flow of the solute than transversely. This anisotropic conductance can also be understood in terms of the interpretation offered in Fig. 22 if one recalls that flow produces an alignment effect on the long-chain anions. Such an alignment in living muscle and nerve cells is created by the pattern of cell growth.

(4) There is now a large collection of self-consistent data in support of *part* of the Bernstein or the Hodgkin–Katz–Goldman equation for the cellular potential:

$$\psi = \frac{RT}{F} \ln \frac{P_K [K^+]_{in} + P_{Na} [Na^+]_{in} + P_{Cl} [Cl^-]_{ex}}{P_K [K^+]_{ex} + P_{Na} [Na^+]_{ex} + P_{Cl} [Cl^-]_{in}} \qquad (16)$$

where P_K, P_{Na}, and P_{Cl} are the K^+-, Na^+- and Cl^--ion permeability constants and $[K^+]_{in}$, $[Na^+]_{in}$, and $[Cl^-]_{in}$ their intracellular concentrations. R and F are the gas and Faraday constants, respectively. The dependence of the potential on the absolute temperature T and its logarithmic relation to the external K^+

and Na^+-ion concentrations have been repeatedly verified (McDonald, 1900; Cowan, 1934; Curtis and Cole, 1942; Ling and Woodbury, 1949; Ling, 1967b, 1962, Chapt. 10). However, attempts to demonstrate a dependence of the potential on the intracellular K^+- and Na^+-ion concentrations have met with contradictory results. Thus injection of highly concentrated salt solutions into squid axons and muscle fibers (Grundfest *et al.*, 1945; Falk and Gerard, 1954), or leaching of K^+ and Na^+ ion from muscle cells, produces none of the changes anticipated on the basis of the membrane theory (Tobias, 1950; Koketsu and Kimura, 1960). Nor does changing the external chloride concentration produce a permanent change in the potential the way changing the external K^+-ion concentration does (Hodgkin and Horowicz, 1959). Other experiments performed both on living muscle cells as well as those model systems that played a major part in the development of the membrane theories of cellular electrical potential (e.g., glass electrodes, collodion electrodes) (Ling, 1960, 1967b, 1962, Chapt. 10) led the reviewer to the conclusion that this potential is in fact not a membrane potential but rather a phase-boundary potential (i.e., a potential arising at the interface of the external solution and the protein–water fixed-charge system; see also Beutner, 1920). As such, this potential is determined by the density and nature of the anionic groups on the proteins of the cell surface. In simplified form the equation for the potential is thus

$$\psi = \text{constant} - \frac{RT}{F} \ln \left(\tilde{K}_K [K^+]_{ex} + \tilde{K}_{Na} [Na^+]_{ex} \right) \qquad (17)$$

where K_K and K_{Na} are the adsorption constants of the K^+ and Na^+ ions on the surface anionic sites. Although this equation has a different basis from the Hodgkin–Katz–Goldman equation, it is formally identical with that part of it which has been experimentally verified. It does not contain those terms relating to the intracellular ionic concentrations or the external Cl^--ion concentration whose relation to the potential has not been verified. The adsorption constants $\tilde{K}_K$ and $\tilde{K}_{Na}$ replace the permeability constants in Eq. (16). According to the association-induction hypothesis, these constants change during excitation because of an all-or-none cooperative change in the c-value of the anionic sites (see Fig. 7). Thus at rest, the c-value is such that $\tilde{K}_K >> \tilde{K}_{Na}$. In consequence, Eq. (17) reduces to

$$\psi_r = \text{constant} - \frac{RT}{F} \ln \tilde{K}_K [K^+]_{ex} \qquad (18)$$

where ψ_r is the potential of the resting cell. This relation has been confirmed over and over again in a large variety of tissues since it was first discovered by McDonald (McDonald, 1900).

During excitation, the c-value shifts to a value such that $K_{Na} > K_K$ and Eq. (17) now approaches

$$\psi_{ac} = \text{constant} - \frac{RT}{F} \ln \tilde{K}_{Na} [Na^+] \tag{19}$$

This relation between the magnitude of the action potential, ψ_{ac} and log $[Na^+]$ was discovered and extensively investigated by Hodgkin and his co-workers (Hodgkin, 1951; Hodgkin and Katz, 1949).

Anticipating work to be presented in a following section, I would like to point out that there is theoretical reason to believe that a local change in the physical state of the water may accompany this c-value shift. Experimental NMR studies by Fritz and Swift (1967) have demonstrated a change in the state of water during depolarization of nerve. Such a change, accompanied by an increase in the Na^+-ion preference of the cell surface sites would contribute to the creation of the action potential profile.

In summary, the failure to demonstrate a consistent correlation between the cellular potential and the intracellular K^+ and Na^+ ion indicates that the cellular electrical potential cannot be construed to be a proof of the membrane theory. In fact, this failure adds very important evidence against it.

D. Molecular Mechanisms in the Integrative Function of Protoplasm

In the preceding sections, we have examined the nature of the protoplasm in terms of the association–induction hypothesis. We have shown that the equilibrium properties of the protein–water fixed-charge system are capable of accounting for most experimental observations concerning solute distribution in living cells. However, living protoplasm is vastly different from sheep's wool or even isolated actomyosin gel. To illustrate this difference let us again consider the bacterial flagellum. This pure protein–water system as it exists on the bacteria is active, a wool fiber is not. On closer examination we find that this activity has the following characteristics: It is the result of a reversible alteration between two states (short and long), the change of state is controlled by a signal received at a distance [from the basal granule, Astbury's signal box (Astbury, 1951)] and the restoration of the flagellum to its original state is energized, also at the basal granule. In the following discussion, we shall examine a theoretical model capable of performing these functions.

1. Two Simple Models

Let us consider a very simple model first. If we join soft iron nails end to end with pieces of string as shown in Fig. 23A, they would distribute themselves in a

random manner and not interact with iron filings strewn around them. If a strong magnet is then brought near the nail at one end, a chain reaction of magnetization occurs ending with all the nails magnetized and the iron filings strongly oriented around the nails. In this process we have demonstrated both energy and information transfer over a distance made possible by the magnetic

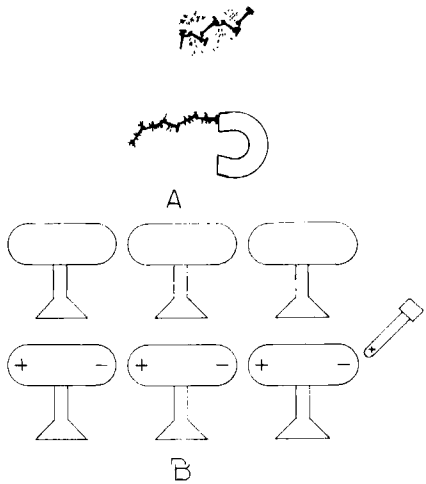

FIG. 23. Two simple moles demonstrating information and energy transfer over distances due to propagated short-range interactions. (A) A chain of soft iron nails joined end to end with pieces of string is randomly arrayed and does not interact with the surrounding iron filings. The approach of a magnet causes propagated alignment of the nails and interaction with the iron filings. (B) Electrons in a series of insulators are uniformly distributed before the approach of the electrified rod, R. Approach of the rod displaces the electrons by induction such that the insulator becomes polarized with regions of low electron density and regions of high electron density.

susceptibilities of soft iron. (If we had used wooden nails, for example, nothing would have happened).

This magnetic model, of course, has its electrical analog (Fig. 23B). An electrically charged rod when brought near a series of closely placed insulators will produce, by induction, alternating negatively and positively charged poles on the insulators. When the electrified rod is removed, the insulators again lose their electrical polarization. Here once more, we have energy and information transfer made possible by a series of closely placed polarizable materials. Depending on the polarizing influence of the electrified rod, there is a redistribution of electrons in the chain of insulators such that localized electron-poor and electron-rich regions are created. These examples illustrate the mechanism of *induction.*

I have suggested as a part of the association-induction hypothesis that the ability of protoplasm to function coherently relies on a fundamentally similar induction mechanism. The polarizable material is, in fact, the polypeptide chain and its appendages, the side chains.

2. *The Basic Mechanism—The Inductive Effect*

Acetic acid (CH_3COOH) is a weak acid. This means that its carboxyl group interacts strongly with a proton in aqueous solution and the fraction of carboxyl groups in the dissociated state is relatively small. Trichloroacetic acid (CCl_3-$COOH$), on the other hand, is a very strong acid. This means that its carboxyl group interacts only weakly with a proton; the fraction of carboxyl groups in the dissociated state is large. Trichloracetic acid is derived by substituting chlorine atoms for the three hydrogen atoms in the methyl group. Since chlorine atoms are more electronegative than hydrogen atoms (i.e., the chlorine atom has a greater propensity to draw electrons toward itself than does the hydrogen atom), this substitution produces a decrease in the electron density of the carboxyl group (i.e., a c-value decrease). Since the energy of interaction between the carboxyl group and the proton is primarily electrostatic in nature, a decrease of c-value leads to a weakening of the interaction energy and more H^+ ion is found in the dissociated state. Thus the substitution of chlorine atoms for hydrogen atoms produces an inductive change in the dissociation constant of an acid group on a different portion of the molecule.

This inductive effect is a general property of organic compounds and its consequences are not limited to a change of acid dissociation constants. Taft, for example, showed that a wide variety of equilibrium and kinetic properties of organic compounds are influenced in a predictable manner by the inductive effects of a long list of substituents including hydrogen and chlorine atoms (Taft, 1960; Taft and Lewis, 1958; Hammett, 1940; Ling, 1964a,b). Among these properties is the strength of the hydrogen bonds formed by many of these compounds (Ling, 1964a,b, 1962, Chapt. 7). Thus substituting a hydrogen atom for a chlorine atom on diethyl ether reduces the electron density of the ether oxygen, and thus lowers its proton-accepting power (Gordy and Stanford, 1941).

3. *How Far Can the Inductive Effect Be Transmitted?*

The dissociation constants of the α-amino and α-carboxyl groups of amino acids

$$(R-\underset{\displaystyle NH_2}{\overset{|}{C}}-COOH)$$

vary because of the varying "electronegativity" of the side chain (R). When

peptides are formed by joining amino acids, and most of the α-carboxyl groups and α-amino groups are transformed into proton-accepting C=O and proton-donating NH groups. However, the α-carboxyl group and α-amino group at the ends of the peptide remain as such. The pK value of these terminal groups in a series of glycine peptides can be studied as an indication of just how far the inductive effect produced by substituting a hydrogen atom by a glycyl group (NH_2CH_2CO) can be transmitted. Table I shows that this substitution has an effect on the α-

TABLE I

	Amino group			Carboxyl group		
	Water		1*M* NaCl	Water		1*M* NaCl
NH_2CH_2COOH	9.70	9.60	9.49	2.42	2.34	3.02
$NH_2CH_2CONHCH_2COOH$	8.20	8.13	8.07	3.13	3.06	3.33
$NH_2(CH_2CONH)_2CH_2COOH$	8.00	7.91	7.83	3.00	3.26	3.39
$NH_2(CH_2CONH)_3CH_2COOH$	7.75	7.75	7.93	3.05	3.05	3.50
$NH_2(CH_2CONH)_4CH_2COOH$	7.70	7.70	—	3.05	3.05	—
$NH_2(CH_2CONH)_5CH_2COOH$	7.60	7.60	—	3.05	3.05	—

carboxyl oxygen even though it is separated from the substituent by one peptide amide group (—CONH—), two saturated carbon atoms, one nitrogen atom, and one carboxyl carbon atom. This example shows that protein chains are unusually polarizable. On this basis, one may anticipate that changes of the "electronegativity" of a side chain, created by the dissociation of a proton for example, may exercise significant influence on its two neighboring CONH groups:

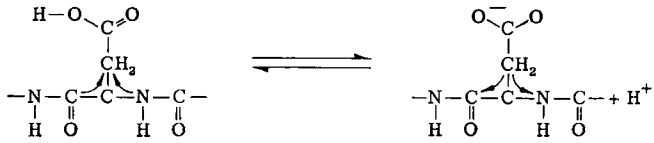

Conversely the *c*-value of the carboxyl group will be changed if the

groups change their H-bonding partners to others of different hydrogen-bonding (or polarizing) strength.

4. The Interplay of Energy and Entropy

The models of magnetized iron nails and electrified insulators deal with macroscopic objects; here energy alone plays a significant role. Phenomena such

as ion adsorption and exclusion are microscopic events. As such, they depend on entropy as well as on energy. A simple example is the sublimation of ice at below-freezing temperatures. Thus both a housewife drying laundry in winter and a biochemist freeze-drying an enzyme depends on the large gain of translational and rotational entropy of the water when the ice vaporizes. From the standpoint of energy alone, such a step is highly unfavorable.

Let us now consider a segment of a polypeptide chain containing m peptides. It can wind itself into, for example, an α-helix or it can become fully extended (a so-called "random coil"). In the helical form all the NHCO groups of the backbone have formed hydrogen bonds with other CONH groups on the same polypeptide chain. These groups are thus internally saturated and shielded from further interaction. In the extended conformation, the NHCO groups are free; in an aqueous medium, they have little choice but to form hydrogen bonds with surrounding water molecules. Let us say that each NHCO group effectively interacts with n water molecules. If we ignore all other components of the chain (i.e., side chains), whether this peptide exists in the helical or the extended form will depend on the total energy and entropy of the entire system. In the *helical state* the energy and entropy terms to be considered are: (1) The energy of a pair of peptide H-bonds; (2) the entropy of the helical peptide; (3) the total energy of the free water involved with each NHCO group; (4) the total entropy of the free water involved with each NHCO group.

Of these four items (2), (3) and (4) are constant for all helical proteins; (1) on the other hand, varies with the nature of the protein molecule. In the *extended state* we must consider: (5) The energy of the peptide $(\text{water})_n$ complex; (6) the entropy of the peptide $(\text{water})_n$ complex. However (5), (6), and the value of n are mutually dependent. Thus if the energy of one peptide–$(H_2O)_n$ complex is known, its entropy as well as n can be defined because the properties of water molecules are unchanging.

In brief, whether the polypeptide exists in the helical state or the extended form essentially depends on the relative magnitudes of the energies of the peptide–peptide bonds and the peptide $(\text{water})_n$ bonds. If these bonds had the same energy in all proteins, of course, one would find them either all in the helical form or all in the extended form. This clearly is not the case. The usual explanation offered for the variability in the conformation of different proteins is the interaction among the side chains and the disruptive influence of proline and hydroxyproline on the formation of the α-helix. Among the side-chain tertiary interactions are: (1) disulfide (S–S) formation; (2) hydrophobic bonds between nonpolar side chains; (3) ionic bonds between charged groups (salt linkages); (4) hydrogen bonds; (5) electrostatic attraction between oppositely charged side chains; (6) electrostatic repulsion between similarly charged side chains.

Of these all except (6) and sometimes (5) favor the formation of the α-helical structure. The electrostatic repulsion can be effectively eliminated if the protein is at its isoelectric point (IEP). Thus if the conventional interpretation is entirely correct, a comparison of the helical stability at the IEP of different proteins should show that those with a large array of functional groups form the strongest helix. Those that are not capable of forming tertiary structure would form the least stable helix. An examination of the properties of a special poly-L-alanine polymer will show that this is not at all the case.

5. *Evidence for the Direct Inductive Influence of the Side Chain on the Strength of the NH · · · OC Bond in the α-Helical Structure*

It is well known that the majority of proteins contain a large number of side chains capable of forming helix-stabilizing tertiary structure. Yet of these proteins some, oxidized ribonuclease, for example, do not form the helical structure in an aqueous medium (Harrington and Schellman, 1956). Many others that do form a helical structure lose it in the presence of 8 *M* urea, 5 *M* quanidine–HCl, or 0.1 *M* dodecyl sodium sulfate. Thus if tertiary interactions are the only factors in stabilizing the α-helix, one would expect that a polypeptide that cannot form any helix-stabilizing tertiary structure would be entirely in the extended conformation. The findings of Doty and Gratzer proved otherwise (Doty and Gratzer, 1962). These authors found that a poly-L-alanine polymer, made water soluble by being connected to two block polymers of poly-D, L-glutamic acid on either end, exists entirely in the form of an α-helix. The stability of this helix is such that it resists all common denaturing agents including 10 *M* urea, 4 *M* guanidine–HCl, and 0.1 *M* dodecyl sodium sulfate. Yet, as Doty and Gratzer point out, this stability cannot be the result of side-chain interaction because the methyl side chains are too short to interact with the nearest neighboring methyl side chains. Since the polypeptide backbone of all proteins and polypeptides is the same, the unusual strength of the poly-L-alanine helix can only be the result of some attribute derived from the properties of the CH_3 side chain. We are therefore compelled to find a new mechanism by means of which the CH_3 group can strengthen the helical structure.

The methyl side chain is an electron-donating substituent (compare the pK values of HCOOH, 3.8; CH_3COOH, 4.75; and CH_3CH_2COOH, 4.87). We have shown earlier that an inductive effect can be transmitted from a side chain at least as far as the two NHCO groups flanking it. From this we must conclude that the proton-donating power of the NH group and the proton-accepting power of the CO group immediately adjacent to the side chain are acted on to different degrees by the inductive effect emanating from the side chain and that the consequence of this electron-donating side chain is to strengthen the helical NH–OC bond.

Let us consider this problem in a greater detail.

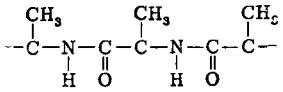

The methyl side chain releases electrons toward both the immediately neighboring C=O and NH groups thereby both strengthening the proton-accepting power of the C=O group and weakening the proton-donating power of the NH group. If these actions were exactly equal in magnitude, it would be hard to understand how the helix could be strengthened because the strength of the CO–HN bond must depend on the proton-accepting power of the CO and the proton-donating power of the NH group. The fact that the helix is strengthened has a dual implication: (1) the proton-accepting power of the CO group is increased more than the proton-donating power of the NH group is decreased and (2) the increase of proton-accepting power of the CO group increases the free energy of the helical CO–HN bond more than that of the CO–$(H_2O)_n$ bond. |One might recall that in Section III, A,3 we showed how a similar increase in the electron density (i.e., *c*-value increase) of the parent group of the CO group, the $-COO^-$ group, also has a differential effect, producing a greater increase in the free energy of association of Na^+ ion than in that of K^+ ion.|

6. *The General Model of Cooperative Adsorption with Emphasis on a Molecular Mechanism of Control and Energy–Information Transfer*

The first statistical-mechanical treatment of a cooperative transition was made by Bragg and Williams (Bragg and Williams, 1934) for the order–disorder transition of β-brass with increasing temperature. More recently, it has been recognized that the denaturation of proteins and DNA also represents a cooperative phenomenon (Schellman, 1955; Zimm and Bragg, 1958; Gibbs and DiMargio, 1958). In all these cases, the nearest-neighbor interaction energy was considered primarily entropic in nature, referring to the increase in entropy as the native helical structure is broken. Our treatment of cooperative phenomena in living cells uses similar statistical-mechanical methods; it differs primarily in that the transition is no longer considered to be between an ordered state and a disordered state but between two alternate states of adsorption which can be ordered or disordered and that the nearest-neighbor interaction has an energy component as well as an entropic component.

Before presenting our general model, it will be useful to define the *c'*-value as a measure of the positive charge of a cationic group (NH_3^+ group). This parameter is analogous to the *c*-value devised to measure the electron density of an anionic oxyacid group. The proton-accepting power of the C=O group and

the proton-donating power of the NH group may also be represented by a c-value analog and a c'-value analog, respectively.

Let us now consider the model of a small segment of a protein chain containing a controlling site (cardinal site) shown in Fig. 24.

The backbone amide groups have two choices of partners, either amide groups on an adjacent protein segment (a^+ a^-) or free hydrogen-bonding molecules such as water (b^+, b^-). In the absence of an adsorbent at the cardinal site, the c-value analogs of the amide CO groups as well as the c'-value analogs of the amide NH groups all have the low value of, say, 1 (see inset). In this state, the electrons are fairly evenly distributed (as in the case of the series of insulators before the electrified rod was brought near, Fig. 23B), and the backbone groups prefer to interact with the fixed groups a^+ and a^- (upper diagram). If a cardinal adsorbent C is then introduced, it reacts with the cardinal site. An inductive effect then raises the c'-value analog of the nearest neighboring NH group from 1 to 2. At this c-value, this site no longer prefers a^- but b^- and an $a^- \rightarrow b^-$ exchange takes place. Because b^- is more polarizing than a^-, the replacement of a^- by b^- has the effect of withdrawing an electron from the neighboring CO group. The c-value analog of this group then rises from 1 to 2 leading to an $a^+ \rightarrow b^+$ exchange. This process continues until all the a^+ and a^- are replaced by b^+ and b^-. The result of the cardinal adsorption is to create in an all-or-none manner a series of water adsorption sites and (Ling, 1962) to cause an all-or-none dissociation from the adjacent protein and the assumption of a new discrete conformation.

If the numerous hydrogen-bonding, ionic, and other sites on a protein molecule were independent, each site would have a large variety of choices in its partner. Such a protein could exist in a variety of conformations not sharply distinguishable from one another. In the present model there is site-to-site interaction between nearest neighbors such that the occupation of neighboring sites by the same adsorbent is favored. This autocooperative interaction leads to the existence of discrete molecular states (conformations) of the protein molecules (see the following section).

It is the basic autocooperative nature of adsorption on proteins that makes possible the modulation and control of many sites by a small number of cardinal adsorbents. Such cardinal adsorbents may be hormones, drugs, ATP, and so forth. Their action and inaction constitute the basic step in energy and information transfer over long distances (Ling, 1962).

7. *A More Specific Model; The Cooperative Adsorption of K^+ and Na^+ Ion*

Figure 25 shows a protein segment carrying anionic side chains existing in two alternative states in an aqueous environment containing both K^+ and Na^+ ion. In one state (B) the carboxyl groups have a relatively low charge density (low

c-value), and prefer K^+ ion over Na^+ ion. The smaller separation of the positive charge of the K^+ ion from the anionic charge of the carboxyl oxygen makes the whole carboxyl-group-K^+-ion complex a weaker electron-donating source than an ionized carboxyl group by itself. Following the finding about poly-L-alanine, we might anticipate a weakening of the helical structure. In consequence, the protein segment is found in the extended form. Water in the close vicinity of the chain exists in the polarized multilayer state.

In the alternative state (A), the anionic side chains are occupied by Na^+ ion, which, as our previous calculations have shown (in the low c-value ranges considered here) tends to assume a configuration in which more water molecules separate the cation from the carboxyl group. The result is that the carboxyl-group-H_2O-Na^+-ion complex functions on the whole as a stronger electron-donating group (than the carboxyl-group-K^+ion complex) thereby stabilizing the helical conformation. The surrounding water molecules in this case would be in a free state. The transition between the two states A and B is controlled by the cardinal adsorbent C.

8. *The Equation for Cooperative Adsorption on Proteins*

An equation based on the method of the one-dimensional Ising model was published for cooperative adsorption on a protein chain by Yang and Ling in 1964 (see Ling, 1964a). In this model, similar sites on a long chain have similar properties and there is nearest-neighbor interaction among these sides. Each site has two choices of adsorbent. For the adsorption of K^+ ion in the presence of Na^+ ion, the equation has the following form (see Ling, 1964a, for the general equation)

$$[K^+]_{ad} = \frac{[f]}{2}\left\{1 + \frac{\xi - 1}{[(\xi - 1)^2 + 4\,\xi \exp(\gamma/RT)]^{1/2}}\right\} \tag{20}$$

where

$$\zeta = \frac{[K^+]_{ex}}{[Na^+]_{ex}} \times \frac{K^\circ_{Na}}{K^\circ_{K}} \tag{21}$$

As one may recall, $[f]$ represents the concentration of the adsorbing sites. K°_{Na} and K°_{K} are the intrinsic adsorption constants of the Na^+ and K^+ ion, respec-

FIG. 24. Diagrammatic illustration of a cooperative transition induced by a cardinal adsorbent. The top figure shows the variation of the free energies of adsorption with changes of the c-value analog of the C=O group and the c'-value analog of the NH group. Figures below demonstrate the stepwise displacement of b^+ and b^- (NH and C=O groups on the lower polypeptide) by a^+ and a^- in consequence of interaction with the cardinal adsorbent at the extreme left. The overall result of the cooperative transition is the dissociation of the two peptides (or the uncoiling of a helix).

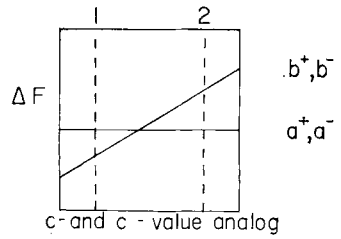
1
2
ΔF
b+,b-
a+,a-
c- and c - value analog

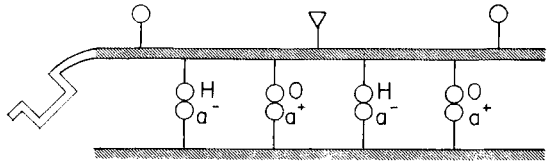
H
a-
O
a+
H
a-
O
a+

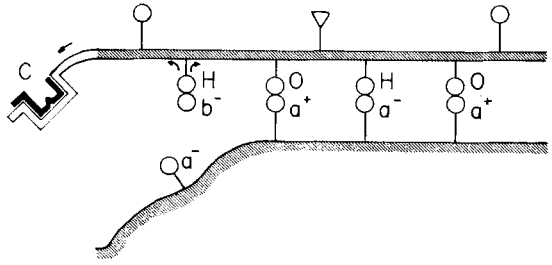
C
H
b-
O
a+
H
a-
O
a+
a-

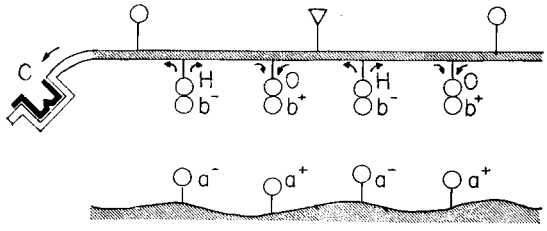
C
H
b-
O
b+
H
b-
O
b+
a-
a+
a-
a+

tively, and are related to the intrinsic standard free energies of adsorption $\Delta F^{\circ\circ}_{Na}$ and $\Delta F^{\circ\circ}_{K}$ by the relation

$$-\Delta F^{\circ\circ}_{Na} = RT \ln K^{\circ}_{Na} \tag{22}$$

$$-\Delta F^{\circ\circ}_{K} = RT \ln K^{\circ}_{K} \tag{23}$$

The free energy of nearest-neighbor interaction is $-\gamma/2$. It is equal to the change in free energy each time a new neighboring pair of dissimilar adsorbents is created. Thus in a series of three adjacent sites all adsorbing Na^+ ion (Na^+, Na^+, Na^+), if the middle site is allowed to change its Na^+ ion for a K^+ ion (Na^+, K^+, Na^+), the total energy change is the difference in the intrinsic free energies ($\Delta F^{\circ\circ}_{K} - \Delta F^{\circ\circ}_{Na}$) *plus* $2(-\gamma/2)$ or $-\gamma$, because of the two new neighboring pairs of Na^+, K^+ created. On the other hand, a shift from Na^+, Na^+, K^+ to Na^+, K^+, K^+ involves only $\Delta F^{\circ\circ}_{K} - \Delta F^{\circ\circ}_{Na}$ since no new Na^+, K^+ neighboring pairs are created.

An important feature of the equation for cooperative adsorption is that if log ($[K^+]_{ad}/[Na^+]_{ad}$) is plotted against log ($[K]_{ex}/[Na]_{ex}$) (as in Fig. 28, for example) the tangent to the resulting curve through the locus at which $[K^+]_{ad}/[Na^+]_{ad} = 1$, is described by the following equation (Ling, 1964a, 1965b, 1966):

$$\log\left(\frac{[K^+]_{ad}}{[Na^+]_{ad}}\right) = n \log\left(\frac{[K^+]_{ex}}{[Na^+]_{ex}}\right) + n \log\frac{K^{\circ}_{K}}{K^{\circ}_{Na}} \tag{24}$$

The slope n is related to the free energy of nearest-neighbor interaction by the explicit relation

$$n = \exp\left(-\frac{\gamma}{2RT}\right) \tag{25}$$

when $n = 1$, $-\gamma/2 = 0$ and there is no nearest-neighbor interaction. In this case, the adsorption is effectively noncooperative and indeed follows the well-known Langmuir adsorption isotherm (Fig. 26). When $n < 1$, $-\gamma/2 > 0$, and the nearest-neighbor interaction is such that dissimilar adsorbents on adjacent sites are favored (i.e., K, Na, K, Na, etc.). We have referred to such interactions as heterocooperative (Ling, 1962, p. 102). If $n > 1$, $-\gamma/2 > 0$; this means that the nearest-neighbor interaction is such that similar adsorbents on adjacent sites are favored (e.g., K^+, K^+, K^+, K^+, or Na^+, Na^+, Na^+, Na^+). Such

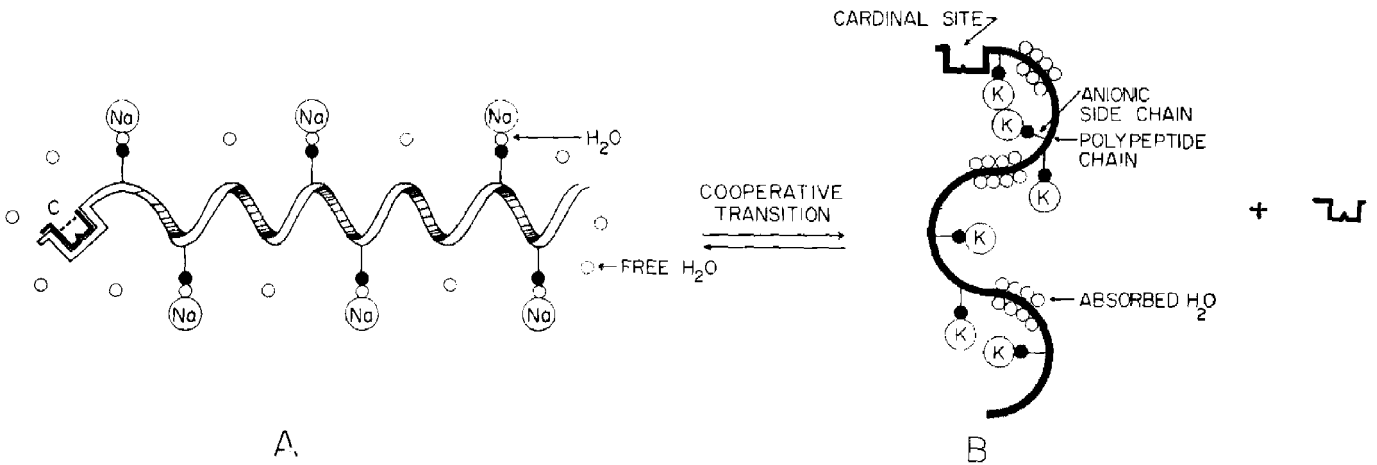

FIG. 25. Diagram of a portion of a protein molecule undergoing autocooperative transformation. For simplicity, adsorbed water molecules in multilayers are shown as a single layer. ⅂⅃-shaped symbol represents a cardinal adsorbent.

interactions are referred to as autocooperative. It is a major theme of the association–induction hypothesis that this type of cooperative adsorption underlies most, if not all, of the all-or-none phenomena known in cell physiology (Ling, 1962, 1964b).

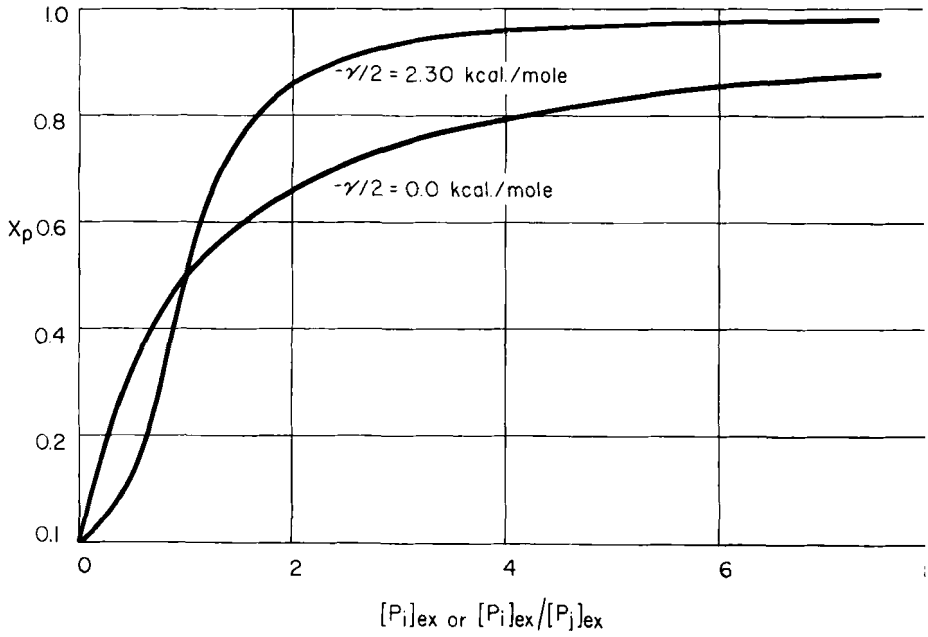

FIG. 26. Cooperative adsorption isotherm for a one-dimensional chain. Linear plots of theoretically calculated isotherms. For $-\gamma/2 = 2.30$ kcal./mole, the isotherm is autocooperative, showing a sigmoid shape. For $-\gamma/2 = 0.0$ kcal./mole (the Langmuir adsorption isotherm), the curve resembles a hyperbola (Ling, 1966b, by permission of *Federation Proceedings*).

9. *The General Equation for Solute Distribution in Living Cells*

Equations (13) and (14) are special equations for K^+- and Na^+-ion distribution in the case in which there is no site-to-site interaction (i.e., adsorption follows the Langmuir adsorption isotherm). The following more general equation for intracellular K^+ ion is valid for the case in which the sites have nearest-neighbor interaction as well:

$$[K^+]_{in} = \alpha q_K [K^+]_{ex} + \sum_{L=1}^{N} \frac{[f]^L}{2} \left\{ 1 + \frac{\xi^L - 1}{[(\xi^L - 1)^2 + 4\xi^L \exp(\gamma^L/RT)]^{1/2}} \right\} \tag{26}$$

where $[f]^L$, ξ^L and γ^L refer to the Lth type of sites. The equation for the intracellular Na^+ ion is

$$[Na^+]_{in} = \alpha q_{Na} [Na^+]_{ex} + \sum_{L=1}^{N} \frac{[f]^L}{2} \left\{ 1 - \frac{\xi^L - 1}{[(\xi^L - 1)^2 + 4\xi^L \exp(\gamma^L/RT)]^{1/2}} \right\} \tag{27}$$

10. Cooperative Adsorption in Biological Systems; Experimental Evidence

Two types of plots are useful in distinguishing cooperative adsorption isotherms from Langmuir adsorption isotherms. We have already mentioned the use of log-log plot, i.e.,

$$\log \frac{[K^+]_{ad}}{[Na^+]_{ad}} \text{ versus } \log \frac{[K^+]_{ex}}{[Na^+]_{ex}}$$

Although the model used in deriving this equation for cooperative adsorption was based on a chain of similar sites, it is often possible to analyze adsorption onto heterogeneous proteins by plotting the data on a log-log plot as if there were only one type of adsorption site. The result appears as a number of straight-line segments joining each other at rather sharp angles (Ling, 1966b). For the combination of isotherms shown in Fig. 27, the outermost segments of the curve have slopes of unity. The two inner segments shift sharply from a slope of less than unity to a slope greater than unity. This shift marks the point at which adsorption changes from heterocooperative to autocooperative.

The linear plot is perhaps more familiar to most biologists. We have shown previously that on such a plot a Langmuir adsorption isotherm has the form of a hyperbola. A cooperative (auto-) curve on the other hand is sigmoid. Such curves are seen in the binding of oxygen onto hemoglobin (Wyman, 1964), in the effect of many feedback inhibitors on enzyme reactions (Monod *et al.*, 1965), and in the adsorption of K^+ ion by living cells (Ling, 1966b). Let us discuss some of these examples in more detail.

a. Oxygen Binding on Hemoglobin. It has long been known that the curve for the binding of oxygen on hemoglobin is not hyperbolic but sigmoid and that this indicates interaction among the four heme groups onto which the oxygen adsorbs (Ling, 1964b, 1966b; Wyman, 1964). A. V. Hill introduced an empirical equation to describe this sigmoid adsorption:

$$\log \frac{y}{1-y} = n \log pO_2 + n \log K_y \tag{28}$$

where y and pO_2 represent the number of adsorbed oxygen molecules per hemo-

globin molecule and the partial pressure of oxygen, respectively, and K_y is a constant (Hill, 1910). It has been known that n is some sort of measure of the degree of interaction. This equation is analogous to Eq. (24). Therefore, the Hill coefficient n is related to the free energy of nearest-neighbor interaction according to Eq. (25). The reaction of oxygen and hemoglobin takes place not in a vacuum but in a water solution. Thus K_y of Eq. (28) is the intrinsic adsorption constant of oxygen divided by the intrinsic adsorption constant of the alternative adsorbent, namely, water.

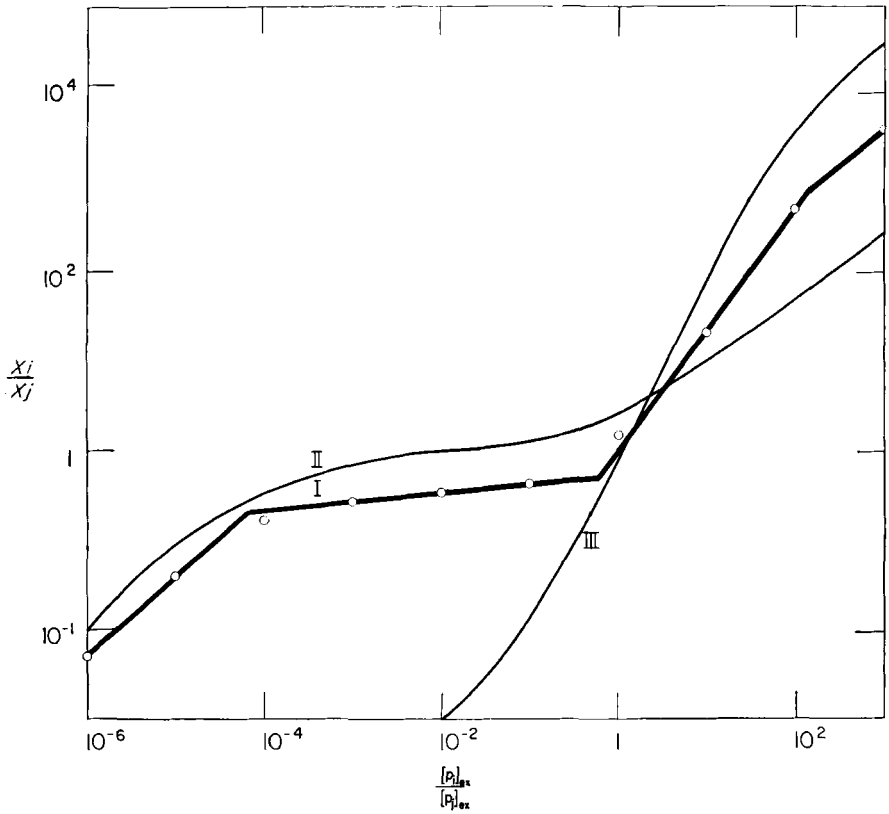

FIG. 27. Complex cooperative adsorption isotherms. Adsorption isotherms for two linear polymers, one autocooperative ($\theta = 100$) and the other heterocooperative ($\theta = 0.1$), are shown, respectively, in curves III and II. Circles represent a complex adsorption isotherm for a mixture containing equal amounts of the above linear polymers and treated as though it contained only a single polymer. Curve I has been drawn as a series of straight lines showing the significant parts of the more exact curve that would join all the circles. Note that the two outermost straight lines have slopes of unity; the slopes of the two middle lines have inexact but significant values which reveal the hetero- or autocooperative nature of the component systems (Ling, 1966b, by permission of *Federation Proceedings*).

If we take account of the fact that there are four heme groups per hemoglobin molecule, the complete equation for oxygen adsorption on hemoglobin becomes:

$$y = 2\left\{1 + \frac{pO_2 \times K_y - 1}{[(pO_2 \times K_y - 1)^2 + 4\,pO_2 \times K_y \exp(\gamma/RT)]^{1/2}}\right\} \tag{29}$$

In Fig. 28, the data of Lyster (see Rossi-Fanelli *et al.*, 1964) for oxygen

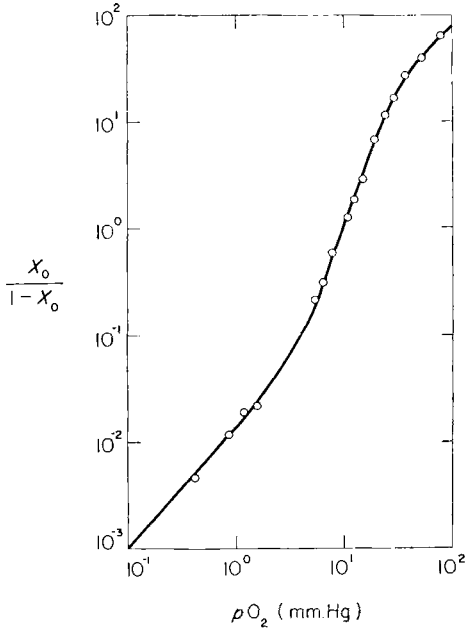

FIG. 28. A log-log plot of the data of Lyster on oxygen uptake by human hemoglobin at pH 7.0 at 19°C. Data of Lyster as presented in the review of Rossi-Fanelli *et al.* (1964). Points are experimental; the line is theoretical according to Eq. (29) with $K = 5.88 \times 10^{-6}\ M$ and $-\gamma/2 = 0.67$ kcal./mole.

binding on hemoglobin have been replotted on a log-log scale. The line is theoretically calculated according to Eq. (29) with K_y equal to $5.88 \times 10^{-6}\ M$ and $-\gamma/2$ equal to 0.67 kcal./mole.

In 1965 Monod, Wyman and Changeux (Monod *et al.*, 1965) presented a model for "allosteric transitions" which, superficially at least, bears some resemblance to our model of cooperative adsorption (see also Haber and Koshland, 1967). A short discussion of their model may help to prevent future confusion. Basically, Monod and his co-workers make the following presuppositions: (1) A protein molecule that is capable of undergoing allosteric transitions contains symmetrical subunits with which ligands react in a symmetrical fashion. (2) This

protein molecule is capable of existing in at least two discrete states which are in equilibrium with each other. (3) The affinity of the protein molecule for the ligand differs in the two states. (4) The binding of any one ligand molecule is independent of the binding of any other. On the basis of this model, Monod and his co-workers are able to predict the types of sigmoid curves seen in allosteric interactions in enzymes (Monod *et al.*, 1965) as well as the curve of Lyster for the binding of oxygen to hemoglobin (see also Changeux *et al.*, 1967).

The model of Monod, Wyman, and Changeux differs from the model presented above in the following ways:

(1) The existence of a small number of discrete states of the protein molecule is an a priori assumption; the reason for the existence of a small number of discrete states rather than a large array of states differing continuously is not made clear. We have pointed out above that it is the nearest-neighbor interaction that gives the protein its capability of assuming such discrete states. Monod *et al.* do not include such nearest-neighbor interaction as a part of their model.

(2) Monod *et al.* refer to "cooperative effects" by which they apparently mean interactions that enhance the binding of substrate molecules; such interactions are thus akin to the autocooperative interactions described above. However, the mechanism they postulate for these effects is not the type of cooperative interaction discussed above, for again nearest-neighbor interactions—an integral part of classic cooperative interactions—are not part of their model.

(3) The Hill coefficient n in the equation for the binding of oxygen to hemoglobin is not related to the parameters (L and c) used by Monod *et al.* to describe their oxygen-binding curves.

(4) In the Monod–Wyman–Changeux model, the change in protein conformation and the binding of single ligands are considered separate events (L and c are independent parameters). The binding of the ligand is not considered to bring about the conformation change. In the model presented above, the binding of the ligand and the change of the protein conformation are interrelated processes not only because of the role of nearest-neighbor interaction but also because the ligands compete for the same sites that maintain the protein conformation.

(5) The Monod–Changeux–Wyman model is only applicable to symmetrical molecules; our model can be applied to all proteins (for experimental data on cooperative adsorption on denatured proteins, see Ling, 1966b).

b. Detergent Binding on Bovine Serum Albumin. There is a fairly large collection of experimental data on *in vitro* adsorption on proteins that are not consistent with the Langmuir adsorption isotherm, but which can be explained on the basis of cooperative adsorption (Ling, 1962). As an example, in Fig. 29 we have replotted the data of Pollansch and Briggs on the adsorption of the

detergent, dodecyl sulfate, on bovine serum albumin. The theory predicts that the point of abrupt change to a higher slope, indicating the beginning of an autocooperative adsorption, should coincide with the beginning of a conformational change. This is indeed the case: At this point the electrophoretic boundary splits from one to two (Pallansch and Briggs, 1954) (for other examples see Ling, 1962).

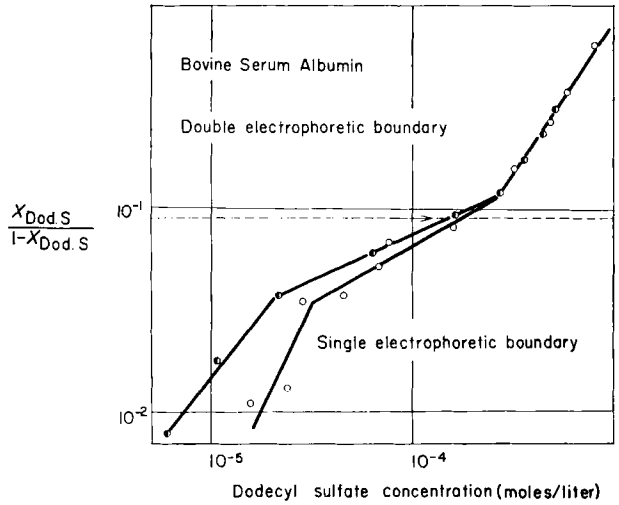

FIG. 29. Adsorption of dodecyl sulfate on bovine serum albumin. Ordinate represents, on a logarithmic scale, the mole fraction of sites binding the anionic detergent, dodecyl sulfate, divided by the mole fraction of sites not binding the detergent. Abscissa represents the dodecyl sulfate concentration also on a logarithmic scale. Total number of binding sites, 102, is the sum of the number of arginin, lysine, and histidine residues per protein molecule. Note that the change from a single to a double electrophoretic boundary (dotted line) occurs at a concentration of dodecyl sulfate corresponding to the abrupt shift of slope from heterocooperative to autocooperative adsorption of detergent. Open and half-filled circles represent two different series of experiments (Pallansch and Briggs, 1954, by permission of *The Journal of American Chemical Society*).

c. Cooperative Adsorption of K+ Ion in Living Cells. i. Frog muscles. It requires 3–4 days of incubation at room temperature for frog muscles to attain new equilibrium ionic concentrations when the external ion concentrations are varied. In our laboratory we have succeeded, by utilizing tissue culture techniques, in maintaining frog muscle in normal condition *in vitro* for 7 days or more, more than long enough to attain these new levels. In Fig. 30 we show the results of an experiment in which the external K^+-ion concentration was varied while the external Na^+-ion concentration remained constant. The equilibrium internal K^+-ion concentrations attained are plotted as a function of the external K^+-ion concentration on a linear plot. The sigmoid curve obtained can be compared with the similar curve obtained for the binding of oxygen by hemoglobin

(Fig. 28). The experimental data have been fitted with a theoretical cooperative adsorption curve [Eq. (20)] calculated using a value of 665 M^{-1} for $K^{\circ}_{K}/K^{\circ}_{Na}$ and of 0.76 kcal./mole for $-\gamma/2$. This means that the adsorption of K^+ is

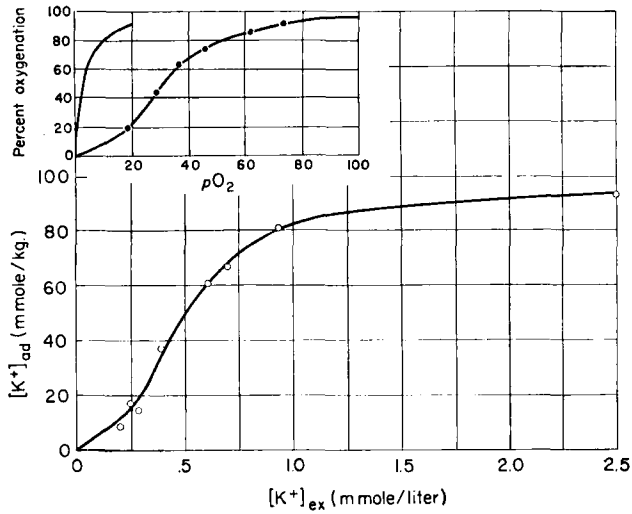

FIG. 30. Equilibrium K^+-ion concentration in frog sartorius muscle in solutions with low K^+-ion concentrations but a high Na^+-ion concentration. Sterily isolated sartorius muscles were shaken for 72 hours at 25°C. in Ringer solutions containing a fixed concentration (100 mmole/liter) of Na^+ ion and varying K^+-ion concentrations. K^+ and Na^+ ion were analyzed by flame photometry on HCl extracts of the muscles. Total intracellular ionic concentration was obtained from raw analytical data after correcting for extracellular space (10%). Adsorbed ionic concentration in millimoles per kilogram of fresh tissue was further computed from the total intracellular concentration by subtracting the interstitial ion concentration (estimated as 10.4% of the equilibrium external ion concentration; this figure represents an average of all values determined to this point). Each point represents a single determination. Inset shows oxygen uptake by human erythrocytes (broken line with filled circles) and by myoglobin (solid line) (from Eastman *et al.*, 1933) (Ling, 1966b, by permission of *Federation Proceedings*).

made more favorable by $2 \times 0.76 = 1.52$ kcal./mole if the two flanking sites are occupied by K^+ ion rather than by Na^+ ion.

ii. Mammalian smooth muscles. Jones has demonstrated that the steady level of K^+-ion uptake in dog arterial smooth muscles also follows Eq. (20) (confirmed by Gulati, to be published). The $K^{\circ}_{K}/K^{\circ}_{Na}$ and $-\gamma/2$ values are, respectively, 93 M^{-1} and 0.61 kcal./mole (Jones and Karreman, in press).

iii. Escherichia coli. Damadian has shown that a sigmoid curve results when the steady level of K^+ ion accumulated in an *E. coli* mutant (RD-2) is plotted against the external K^+-ion concentration in the range of 0–0.3 m*M* external K^+ ion. At higher concentrations there appear to be a second set of cooperative adsorption sites (Damadian, 1968).

11. The Control and Energization of Cooperative Adsorption

a. The Control of K-Na Adsorption by Cardiac Glycosides. The theoretical model shown in Fig. 2 predicts that in the same ionic environment the interaction of the protein with a cardinal adsorbent may shift the system from a relative affinity for K^+ ion to a relative affinity for Na^+ ion in all-or-none manner. Figure 31 shows that the cardiac glycoside lanoxin, at pharmacological concentrations, produces a shift in the cooperative adsorption isotherm such that the ratio of the intrinsic equilibrium constants (K°_K / K°_{Na}) shifts toward a lower K^+-ion preference and a higher Na^+-ion preference by a factor of 20. The autocooperative nature of the curve (slope > 1 at $[K^+]_{ad}/[Na^+]_{ad} = 1$) is preserved.

This effect has profound physiological significance. The sigmoid curve shown in Fig. 30 shows that the muscle can change in a more or less all-or-none manner from adsorbing all K^+ ion to adsorbing all Na^+ ions. However, under physiological conditions, there are no large changes in the plasma concentrations of K^+

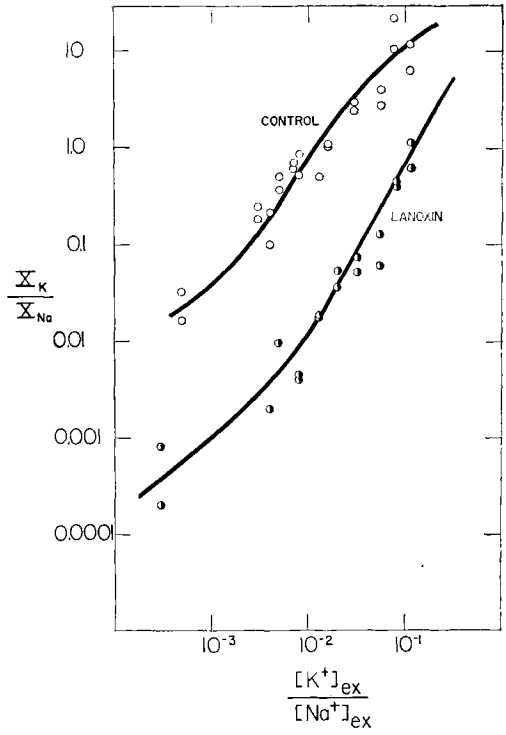

FIG. 31. Log-log plot of the K^+- and Na^+-ion distribution in frog sartorius muscles in the absence (left) and presence of lanoxin. The experimental procedures used were similar to those described in Fig. 30. The lanoxin concentration was 2.5 μg./ml. X_K and X_{Na} refer to mole fraction of adsorbed K^+ and Na^+ ion, respectively.

or Na^+ ions. Under these conditions, changes in adsorbents must be brought about by another agent, preferably one that is active in very small quantities and can influence the adsorbents on a large number of sites by itself. In the present experiment lanoxin is such an agent. Thus in an unvarying ionic environment, interaction with lanoxin changes the site from a state in which K^+ ion is the main adsorbent to one in which Na^+ ion is the main adsorbent. A similarly controlled all-or-none shift of the K^+ and Na^+-ion preference of the anionic sites on the surface of excitable tissues has been discussed at some length in Section III, C.

b. Energization of the Biological Activators. In the history of biology, one of the most admirable events in the 1930's was the way the leaders in the field of metabolism, A. V. Hill and O. Meyerhof, responded to the findings of the then relatively unknown Lundsgaard. In contradiction to the lactic acid theory of muscle contraction proposed by Hill and Meyerhof, Lundsgaard found that muscle could contract in the complete absence of lactic acid production (Lundsgaard, 1930; Henriques and Lundsgaard, 1931). The immediate confirmation of Lundsgaard's finding in Meyerhof's laboratory led Hill to write an article, entitled "A Revolution in Muscle Physiology" (Hill, 1932) which paved the way for the recognition of the important role of ATP in cell function. Subsequent development of the concept of the high-energy phosphate bond led to the postulation that the enzymic hydrolysis of this bond liberates energy for the performance of biological work (Lipmann, 1941). However, the demonstration that the enthalpy (see footnote 3) of the high-energy phosphate bond is not 12 kcal./mole as it was one time thought to be (for a possible source of this error, see Ling, 1962), but only 4.7 kcal./mole (no higher than an ordinary phosphate bond, Podolsky and Kitzinger, 1955; Betzinger and Morales, 1956), has left this theory of the energization of biological work untenable.

In terms of the association–induction hypothesis, ATP is conceived to perform its energization function, not through hydrolytic cleavage, but through adsorption on cardinal sites producing or maintaining a particular cooperative state of the cellular protein (Ling, 1962). The unusually high enthalpy of the adsorption of ATP on G-actin [—24 kcal./mole (Asakura, 1961)] indicates that energization could be accomplished in this manner. The effect of ATP on K^+-ion adsorption would be essentially similar to the demonstrated effect of lanoxin but in the reverse direction.

A prediction of this model is that the K^+-ion concentration in living cells is not dependent on the rate of ATP hydrolysis, but instead is determined by the concentration of ATP per se in the cell. Thus each time an ATP molecule adsorbs on a cardinal site, a fixed number of anionic sites (see Fig. 25) will cooperatively adsorb K^+ ion. Without ATP as the cardinal adsorbent, some other ionic components will occupy the anionic sites; these may be Na^+ ion or fixed cations on nearby proteins. This prediction has been confirmed for K^+-ion

distribution in frog muscle treated with iodoacetate and nitrogen, in human erythocytes, and in *E. coli* (Ling, 1962, Chapt. 9). Figure 32 shows the K+-ion concentration in frog muscles as a function of the cellular ATP concentration.

Once the dependence of K+-ion accumulation on ATP adsorption is realized,

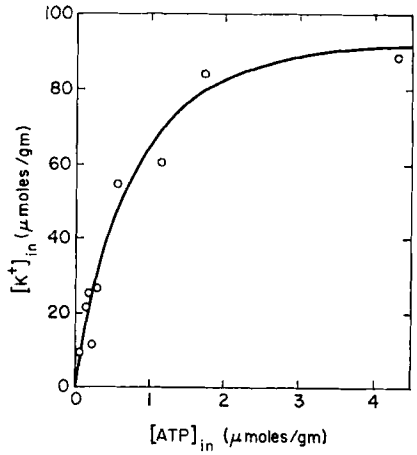

FIG. 32. The correlation of intracellular K+-ion concentration and ATP concentration in frog voluntary muscles. Muscles were treated with 4 m*M* iodoacetic acid for varying lengths of time at room temperature, then chilled in the same bathing solution to 0°C. and allowed to equilibrate at this lower temperature for 1 hour, after which they were analyzed for both their K+ ion and ATP contents (Ling, 1962, by permission of Blaisdell Press).

the physiological role of ATP once more becomes understandable. Thus the normal resting cell hydrolyzes ATP slowly, but the activated cell hydrolyzes ATP very rapidly. (This indicates that the ATPase activity itself is under physiological control.) A cyclic event can be visualized as follows:

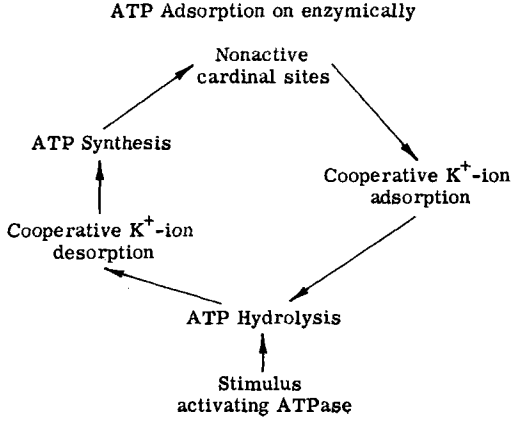

ACKNOWLEDGMENTS

The preparation of this review and the new investigations reported were supported by the National Science Foundation Research Grants GB3921, GB7095, the National Institute of Health Research Grants 2R01-GM11422-04 and HE-07762-64, and the Office of Naval Research Grant Nonr 4371 (00)-105327.

The author is supported by Public Health Service Research Career Development Award K3-GM-19032.

The author thanks Dr. Frank Elliott, Dr. Margaret C. Neville, Margaret M. Ochsenfeld, Grace Bohr, and Marie Bowers for their invaluable help; and the John A. Hartford Foundation for providing the basic equipment for the investigations.

REFERENCES

Asakura, S. (1961). *Arch. Biochem. Biophys.* **92**, 140.
Astbury, W. T. (1951). *Sci. Am.* **184**, 21.
Avery, O. T., MacLeod, C. M., and McCarty, M. (1944). *J. Exptl. Med.* **79**, 137.
Bennett, H. S. (1956). *J. Biophys. Biochem. Cytol.* **2**, Suppl., 99.
Bernstein, J. (1902). *Arch. Ges. Physiol. Pfluegers* **92**, 521.
Betzinger, R. J., and Morales, M. F. (1956). *J. Biol. Chem.* **218**, 945.
Beutner, R. (1920). "Die Entstehung electrischer Ströme in lebenden Geweben und ihre Künstliche Nachahmung durch synthetische organische Substanzen." Enke, Stuttgart.
Boyle, P. J., and Conway, E. J. (1941). *J. Physiol.* (*London*) **100**, 1.
Bradley, S. (1936). *J. Chem. Soc.* p. 1799.
Bragg, W. L., and Williams, E. J. (1934). *Proc. Roy. Soc.* (*London*) **A145**, 699.
Bratton, C. B., Hodgkin, A. L., and Weinberg, J. W. (1965). *Science* **147**, 738.
Bregman, J. I. (1953). *Ann. N.Y. Acad. Sci.* **57**, 125.
Bütschli, O. (1894). "Investigations on Microscopic Foams and on Protoplasm" (E. A. Minchin, transl.). Black, London.
Bull, H. (1944). *J. Am. Chem. Soc.* **66**, 1499.
Chambers, R., and Hale, H. P. (1932). *Proc. Roy. Soc.* (*London*) **B110**, 336.
Chambers, R., and Kao, C. Y. (1952). *Exptl. Cell Res.* **3**, 564.
Changeux, J., Thiery, J., Tung, Y., and Kittel, C. (1967). *Proc. Natl. Acad. Sci. U.S.* **57**, 335.
Chapman, G., and McLauchlan, K. A. (1967). *Nature* **215**, 391.
Cole, K. S. (1932). *J. Cellular Comp. Physiol.* **1**, 1.
Collander, R. (1949). *Physiol. Plantarum* **2**, 300.
Collander, R., and Bärlund, H. (1933). *Acta Botan. Fennicae* **11**, 1.
Conway, E. J. (1946). *Nature* **157**, 715.
Cope, F. (1967). *J. Gen. Physiol.* **50**, 1353.
Cowan, S. L. (1934). *Proc. Roy. Soc.* (*London*) **B115**, 216.
Curtis, H. J., and Cole, K. S. (1942). *J. Cellular Comp. Physiol.* **19**, 135.
Damadian, R. (1968). *J. Bacteriol.* **95**, 113.
Davson, H., and Danielli, J. F. (1952). "The Permeability of Natural Membranes," 2nd Ed. Cambridge Univ. Press, London and New York.
Dawson, D. M. (1966). *Biochim. Biophys. Acta* **113**, 144.
Dean, R. B. (1941). *Biol. Symp.* **3**, 331.
de Boer, J. H., and Zwikker, C. (1929). *Z. Physik. Chem.* (*Leipzig*) **B3**, 407.
De Vries, H. (1885). *Jahrb. Wiss. Botan.* **16**, 465.

Doty, P., and Gratzer, W. B. (1962). *In* "Polyamino Acids, Polypeptides and Proteins" (M. A. Stahmann, Ed.), p. 111. Univ. of Wisconsin Press, Madison, Wisconsin.
Eastman, N. J., Geiling, E. M. K., DeLander, A. M. (1933). *Bull. Johns Hopkins Hosp.* **53**, 246.
Eisenman, G. (1961). *Membrane Transport Metab., Proc. Symp., Prague* (A. Kleinzeller and A. Kotyk, eds.), p. 163. Czechoslovak Academy of Science, Prague.
Eisenman, G., Rudin, D. O., and Casby, J. U. (1957). *Science* **126**, 831.
Epstein, E., and Hagen, C. E. (1952). *Plant. Physiol.* **27**, 457.
Falk, G., and Gerard, R. W. (1954). *J. Cellular Comp. Physiol.* **43**, 393.
Fenichel, I. R., and Horowitz, S. B. (1963). *Acta Physiol. Scand.* **222**, 1.
Fischer, H., and Moore, G. (1908). *Am. J. Physiol.* **20**, 330.
Fritz, O. G., and Swift, T. J. (1967). *Biophys. J.* **7**, 675.
Gibbs, J. H., and DiMargio, E. A. (1958). *J. Chem. Phys.* **28**, 1247.
Gordy, W., and Stanford, S. C. (1941). *J. Chem. Phys.* **9**, 204.
Grundfest, H., Kao, C. Y., and Altamirano, M. (1945). *J. Gen. Physiol.* **38**, 245.
Haber, J. E., and Koshland, D. E. (1967). *Proc. Natl. Acad. Sci.* **58**, 2087.
Hallett, J. (1965). *Federation Proc.* **24**, S–34.
Hamburger, H. J. (1889). *Z. Biol.* **26**, 414.
Hammett, L. P. (1940). "Physical Organic Chemistry." McGraw-Hill, New York.
Harkins, W. D. (1945). *Science* **102**, 292.
Harrington, W. F., and Schellman, J. A. (1956). *Compt. Rend. Trav. Lab. Carlsberg, Ser. Chim.* **30**, No. 6, 21.
Harris, E. J. (1950). *Trans. Faraday Soc.* **334**, 872.
Harris, E. J., and Burn, G. P. (1949). *Trans. Faraday Soc.* **45**, 508.
Heckmann, K. (1953). *Naturwissenschaften* **40**, 478.
Henriques, V., and Lundsgaard, E. (1931). *Biochem. Z.* **236**, 219.
Heppel, L. A. (1940). *Am. J. Physiol.* **128**, 449.
Hermann, L. (1879). "Handbuch der Physiologie," Vol. 2 (F. C. W. Vogel, ed.), p. 3. L. Hermann, Leipzig.
Hill, A. V. (1910). *J. Physiol. (London)* **40**, iv–vii.
Hill, A. V. (1930). *Proc. Roy. Soc. (London)* **B106**, 477.
Hill, A. V. (1932). *Physiol. Rev.* **12**, 56.
Hinke, J. A. M. (1959). *Nature* **184**, 1257.
Hodgkin, A. L. (1951). *Biol. Rev. Cambridge Phil. Soc.* **26**, 339.
Hodgkin, A. L., and Horowicz, P. (1959). *J. Physiol. (London)* **148**, 127.
Hodgkin, A. L., and Katz, R. D. (1949). *J. Physiol. (London)* **108**, 37.
Hodgkin, A. L., and Keynes, R. D. (1953). *J. Physiol. (London)* **119**, 513.
Holter, H., and Holtzer, H. (1959). *Exptl. Cell Res.* **18**, 421.
Holwill, M. E. J., and Burge, R. E. (1963). *Arch. Biochem. Biophys.* **101**, 249.
Horowicz, P., and Hodgkin, A. (1957). *J. Physiol. (London)* **145**, 405.
Huxley, H. E. (1957). *J. Biophys. Biochem. Cytol.* **3**, 631.
Jacques, M. (1936). *J. Gen. Physiol.* **19**, 397.
Jones, A., and Karreman, G. (1969). *Biophys. J.* (in press).
Keynes, R. D., and Maisel, G. W. (1945). *Proc. Roy. Soc. (London)* **B142**, 383.
Koketsu, K., and Kimura, Y. (1960). *J. Cellular Comp. Physiol.* **55**, 239.
Krogh, A. (1946). *Proc. Roy. Soc. (London)* **B133**, 140.
Langmuir, I. (1917). *J. Am. Chem. Soc.* **39**, 1848.
Levi, H., and Ussing, H. H. (1948). *Acta Physiol. Scand.* **16**, 232.
Lewis, M. S., and Saroff, H. A. (1957). *J. Am. Chem. Soc.* **79**, 2112.

Ling, G. N. (1951). *Am. J. Physiol.* **167**, 806.
Ling, G. N. (1952). *In* "Phosphorus Metabolism" (W. D. McElroy and B. Glass, eds.), Vol. 2, p. 748. Johns Hopkins Press, Baltimore, Maryland.
Ling, G. N. (1955). *J. Phys. Med.* **34**, 89.
Ling, G. N. (1960). *J. Gen. Physiol.* **43**, Suppl., 149.
Ling, G. N. (1962). "A Physical Theory of the Living State." Ginn (Blaisdell), Boston, Massachusetts.
Ling, G. N. (1964a). *Biopolymers, Symp.* **1**, 91.
Ling, G. N. (1964b). *Texas Rept. Biol. Med.* **22**, 244.
Ling, G. N. (1965a). *Ann. N.Y. Acad. Sci.* **125**, 401.
Ling, G. N. (1965b). *Federation Proc.* **24**, Suppl. 15, S–103.
Ling, G. N. (1965c). *Perspectives Biol. Med.* **9**, 87.
Ling, G. N. (1966a). *Ann. N.Y. Acad. Sci.* **137**, 837.
Ling, G. N. (1966b). *Federation Proc.* **25**, 958.
Ling, G. N. (1967a). *In* "Glass Electrodes for Hydrogen and Other Cations" (G. Eisenman, ed.). Dekker, New York.
Ling, G. N. (1967b). *Naturw. Rundschau* **20**, 415.
Ling, G. N. (1967c). *In* "Thermobiology" (A. Rose, ed.), Chapt. 2. Academic Press, New York.
Ling, G. N., and Ochsenfeld, M. (1965). *Biophys. J.* **5**, 777.
Ling, G. N., and Ochsenfeld, M. M. (1966). *J. Gen. Physiol.* **49**, 819.
Ling, G. N., Ochsenfeld, M. M., and Karreman, G. (1967). *J. Gen. Physiol.* **50**, 1807.
Ling, G. N., and Ochsenfeld, M. M. (1968a). *Federation Proc.* **27**, 702.
Ling, G. N., and Ochsenfeld, M. M. (1968b). *Proc. Intern. Physiol. Congr. Washington D.C.,* **24**, 266.
Ling, G. N., and Woodbury, J. W. (1949). *J. Cellular Comp. Physiol.* **34**, 407.
Lipmann, F. (1941). *Advan. Enzymol.* **1**, 99.
Lundsgaard, E. (1930). *Biochem. Z.* **227**, 51.
McBain, J. W., and Peaker, C. R. (1930). *J. Phys. Chem.* **34**, 1033.
McDonald, J. S. (1900). *Proc. Roy. Soc. (London)* **67**, 310.
McLaren, A. D., Jensen, W. A., and Jacobson, L. (1960). *Plant. Physiol.* **35**, 549.
Mellon, S. R., and Hoover, E. F. (1950). *J. Am. Chem. Soc.* **72**, 2562.
Mond, R., and Netter, H. (1930). *Pfluger's Arch.* **224**, 702.
Monod, J., Wyman, J., and Changeux, J. (1965). *J. Mol. Biol.* **12**, 88.
Mysels, K. J., and McBain, J. W. (1948). *J. Colloid Sci.* **3**, 45.
Nielsen, J. M., Adamson, A. W., and Cobble, J. W. (1952). *J. Am. Chem. Soc.* **74**, 446.
Osterhout, W. J. V. (1936). *Bacteriol. Rev.* **2**, 283.
Overton, E. (1899). *Vierteljahrsschr. Naturforsch. Ges. (Zürich)* **44**, 88.
Overton, E. (1907). *In* "Handbuch der Physiologie des Menschen" (W. Nagel, ed.), Vol. 2, p. 744. Vieweg, Braunschweig.
Pallansch, M. J., and Briggs, D. R. (1954). *J. Am. Chem. Soc.* **76**, 1396.
Pfeffer, W. (1921). "Osmotische Untersuchungen," 2nd Ed. Engelmann, Leipzig.
Podolsky, R. J., and Kitzinger, C. (1955). *Federation Proc.* **14**, 115.
Rapatz, G., and Luyet, B. J. (1958). *Biodynamica* **8**, 121.
Rossi-Fanelli, A., Antonini, E., and Caputo, A. (1964). *Advan. Protein Chem.* **19**, 73.
Rotunno, C. A., Kowalewski, V., and Cereijido, M. (1967). *Biochim. Biophys. Acta* **135**, 170.
Ruhland, W., and Hoffman, C. (1925). *Planta* **1**, 1.
Ryser, H. J. P. (1968). *Science* **159**, 390.

Schellman, J. A. (1955). *Compt. Rend. Trav. Lab. Carlsberg, Ser. Chim.* **29**, 15.
Schwindewolf, U. (1953). *Naturwissenschaften* **40**, 435.
Starr, M. P., and Williams, R. C. (1952). *J. Bacteriol.* **63**, 701.
Steinbach, H. B. (1940). *J. Biol. Chem.* **133**, 695.
Taft, R. W. (1960). *J. Phys. Chem.* **64**, 1805.
Taft, R. W., and Lewis, I. C. (1958). *J. Am. Chem. Soc.* **80**, 2436.
Tobias, J. M. (1950). *J. Cellular Comp. Physiol.* **36**, 1.
Troschin, A. S. (1958). "Das Problem der Zellenpermeabilitat." Fischer, Jena.
Weibull, C. (1960). *In* "The Bacteria" (I. C. Gunsalus and R. Y. Stanier, eds.), Vol. 1, Chapt. 4. Academic Press, New York.
Wyman, J. (1964). *Advan. Protein Chem.* **19**, 223.
Zierler, K. (1958). *Ann. N.Y. Acad. Sci.* **75**, 227.
Zimm, B. H., and Bragg, J. K. (1958). *J. Chem. Phys.* **28**, 1246.